Machine Learning in Stream/River Water Temperature Modeling: a review and metrics for evaluation

Claudia R. Corona[1], Terri S. Hogue[1,2]

[1]Department of Civil and Environmental Engineering, Colorado School of Mines, Golden, 80401, United States
5   [2]Hydrologic Science and Engineering Program, Colorado School of Mines, Golden, 80401, United States

Correspondence to: Claudia R. Corona (Claudia.corona@mines.edu)

Abstract. As climate change continues to affect stream/river (henceforth stream) systems worldwide, stream water temperature (SWT) is an increasingly important indicator of distribution patterns and mortality rates among fish, amphibians, and macroinvertebrates. Technological advances tracing back to the mid-20th century have improved our ability
10 to measure SWT at varying spatial and temporal resolutions for the fundamental goal of better understanding stream function and ensuring ecosystem health. Despite significant advances, there continue to be numerous stream reaches, stream segments and entire catchments that are difficult to access for a myriad of reasons, including but not limited to physical limitations. Moreover, there are noted access issues, financial constraints, and temporal and spatial inconsistencies or failures within situ instrumentation. Over the last few decades and in response to these limitations, statistical methods and physically based
15 computer models have been steadily employed to examine SWT dynamics and controls. Most recently, the use of artificial intelligence, specifically machine learning (ML) algorithms, has garnered significant attention and utility in hydrologic sciences, specifically as a novel tool to learn undiscovered patterns from complex data and try to fill data streams and knowledge gaps. Our review found that in the recent five years (2020–2024), a similar number (27) of publications using ML, as were published in the previous 20 years, (2000–2019), totaling 54. The aim of this work is three-fold: first, to provide
20 a concise review of the use of ML algorithms in SWT modeling and prediction, second, to review ML performance evaluation metrics as it pertains to SWT modeling and prediction and find the commonly used metrics and suggest guidelines for easier comparison of ML performance across SWT studies and third, to examine how ML use in SWT modeling has enhanced our understanding of spatial and temporal patterns of SWT and examine where progress is still needed.

1 Introduction

Water temperature in a stream/river plays a vital role in nature and society, regulating dissolved oxygen concentrations (Poole & Berman, 2001), biochemical oxygen demand rates, and chemical toxicities (Cairns et al., 1975; Patra et al., 2015). Additionally, SWT is an important indicator of cumulative anthropogenic impacts on lotic environments (Risley et al.,

30 2010). Observations of SWT changes over time can reveal the effects of stream flow regulation, riparian alteration (Johnson & Jones, 2000), and large-scale climate change (Barbarossa et al., 2021) on local ecosystems. From an ecological standpoint, SWT strongly influences (Ward, 1998) the health, survival, and distribution of freshwater fish (Ulaski et al., 2023; Wild et al., 2023), amphibians (Rogers et al., 2020) and macroinvertebrates (Wallace & Webster, 1996). As climate change progresses, SWT will be an increasingly critical proxy for ecosystem health and function, both locally and nationally.

35 ### 1.1 SWT modeling in the 21st century

Technological advances since the turn of the 20th century have improved our ability to measure SWT in an affordable and dependable manner at varying spatial and temporal resolutions (Benyahya et al., 2007; Dugdale et al., 2017). Despite significant advances in the last 100 years, there remain many stream reaches, stream segments and entire catchments that are difficult to access for a myriad of reasons (Ouellet et al., 2020), including, but not limited to physical limitations: i.e.,

40 streams may be in private property, remote or dangerous-to-access areas, financial constraints: access may be limited by monetary resources or lack-there-of, or temporal limitations such as uncertainties/inconsistencies in the continuity of measurements or unforeseen equipment loss/failure (Webb et al., 2008, Isaak, 2011). In response to these limitations, statistical methods and physically based computer models have been steadily employed over the last few decades to support the advancement of scientific understanding of stream form and function and subsequent implications for water management

45 (Cluis et al., 1972, Caissie et al., 1998, Mohseni et al., 1998, Isaak, 2011, Hill et al., 2013, DeWeber and Wagner, 2014). Aided by the continued development of computers and the internet, physical and statistical computer models have gained prominence outside of academia and are more commonly being used by stakeholders and local groups to address a myriad of hydrology challenges (Maheu et al., 2016; Liu et al., 2018; Tao et al., 2020; Rogers et al., 2020). At the same time, the problem-solving success of machine learning (ML), which falls under the umbrella of artificial intelligence, has become

50 increasingly popular in hydrologic sciences in the last few years (DeWeber & Wagner, 2014; Xu & Liang, 2021). Artificial intelligence (AI) describes technologies that can incorporate and assess inputs from an environment, create reasonable choices, and implement actions to meet stated objectives or performance metrics (Xu & Liang, 2021; Varadharajan et al., 2022). As a subset of AI, the goal of ML algorithms and models is to learn patterns from complex data (Friedberg, 1958). A global call to better predict and prepare for near- and far-future hydrologic conditions has led researchers in the last few

55 decades to use ML algorithms to model hydrologic processes at various temporal and spatial scales (Poff et al., 1996; Solomatine et al., 2008; Cole et al., 2014; Khosravi et al., 2023). For example, a type of ML called artificial neural networks (ANNs), have been used since the 1990s in many subfields of hydrology, such as streamflow predictions (Karunanithi et al.,

1994; Poff et al., 1996), rainfall-runoff modeling (Hsu et al., 1995; Shamseldin, 1997), subsurface flow and transport (Morshed & Kaluarachchi, 1998), and flood forecasting (Thirumalaiah & Deo, 1998). For SWT modeling however, the use of ML algorithms such as ANNs have only recently garnered interest (Zhu & Piotrowski, 2020).

1.2. Study Objective

The current work includes an extensive literature review of studies that used ML algorithms/models for river/SWT modeling, hindcasting and forecasting. Our review includes papers cited by Zhu and Piotrowski (2020), who previously conducted a study of ANNs used in SWT modeling, however, we provide a comprehensive examination of peer-reviewed journals that use any type of artificial intelligence/ML algorithm to model or evaluate river/SWT. This review's first objective is to provide a concise review of ML algorithm use in SWT modeling. Secondly, our goal is to examine the ML performance evaluation metrics used in SWT modeling and find the most-used metrics and suggest guidelines for clearer comparison of ML performance. The third objective is to discuss the community's use of ML to address physical system understanding in SWT modeling. Overall, this review aims to serve as a critical assessment of the state of SWT understanding given the increasing popularity of ML use in SWT modeling.

2 Overview: Stream Water Temperature Model Types

2.1 SWT statistical (also stochastic or empirical) models

In the 1960s, considerable interest grew in the prediction of SWT, particularly in the western United States (U.S.) due to increased awareness of environmental quality issues (Ward, 1963; Edinger et al., 1968; Brown, 1969). The creation of large dams, daily release of heated industrial effluents, growing agricultural waste discharge and forest clear-cutting could influence downstream SWT. However, the extent of such influence remained poorly understood and difficult to test at large spatial and temporal scales (Brown, 1969). From the 1960s to the 1970s, understanding of the relationship between SWT and ambient air temperature (AT) was solidified, and scientists began to increasingly use statistical methods to examine the air-water relationships in stream environments (Morse, 1970; Cluis, 1972). Statistical (also stochastic or empirical) models are governed by empirical relations between SWT and their predictors, which requires fewer input data. An example of such progress took place in Canada, where researchers created an autoregressive model to calculate mean daily SWT fluctuations using six months of data from the summer and winter months of 1969 (Cluis, 1972). Cluis (1972) further said that their model was transferrable to other streams of comparable size. The use of statistical methods in SWT modeling became increasingly common in the latter half of the 20th century due in large part to minimal data requirements (Benyahya et al., 2007). For example, scientists in Europe used limited data and statistics to examine the influence of atmospheric and topographic factors on the temperature of a small upland stream (Smith and Lavis, 1975). In Australia, scientists interested in finding limits for reaches of streams downstream from thermal discharges, found a simple method that could predict SWT based solely on-site altitude and AT or upstream SWT (Walker and Lawson, 1977). In Canada, SWT was predicted using a

stochastic approach, which included the use of Fourier series, multiple regression analysis, Markov processes, and a Box-
90   Jenkins time-series model (Caissie et al., 1998). In the 21st century, statistical methods continue to be a prominent tool used
for SWT modeling and prediction (Ahmadi-Nedushan et al., 2007; Chang and Psaris, 2013; Segura et al., 2015; Detenbeck et
al., 2016; Siegel and Volk, 2019; Ulaski et al., 2023; Fuller et al., 2023). We refer the reader to Benyahya et al. (2007) for a
comprehensive review of SWT statistical models and approaches.

2.2 SWT physically based (also process-based, deterministic, mechanistic) models

95   While statistical methods can be straightforward to use and requires minimal in situ data for first analysis (Benyahya et al.,
2007), limitations and uncertainty with regards to SWT predictions is possible, specifically when trying to understand the
controls of energy transfer mechanisms responsible for trends (Dugdale et al., 2017). To address these shortcomings and
with the introduction of personal computers in the late 1960s (Dawdy & Thompson, 1967), researchers developed computer
models and software programs that tried to address the more fundamental hydrology questions founded in physics and
100 natural processes (Theurer et al., 1985; Bartholow, 1989). One example of such progress was a SWT prediction one-
dimensional computer model that used a simplified energy conservation equation to predict SWT for the upper reaches of the
Columbia River in the Pacific Northwest of the U.S., during July 1966 (Morse, 1970). These models are described as being
physically based or process-based (alternatively called 'deterministic' or 'mechanistic' models).

Due to the continued lack of sufficient in situ observations and resources with which to undertake field studies in SWT
105 science (Dugdale et al., 2017), physically based models became increasingly used. From the end of the 20th century through
the present, they are considered one of the best available options in generating predictions of SWT, particularly at a localized
scale (Dugdale et al., 2017). Physically based models became useful enough that government agencies introduced their own
models to encourage uniformity. In the 1980s, the U.S. Geological Survey (USGS) introduced a physically based model that
simulated SWT called SNTemp (Theurer et al., 1985; Bartholow, 1989). A few years later, the U.S. Environmental
110 Protection Agency (EPA) introduced SHADE-HSPF for similar purposes (Chen, Carsel, et al., 1998; Chen, McCutcheon, et
al., 1998). Where available, academic scientists coupled field measurements with physically based numerical models. For
example, scientists in Minnesota created a numerical model, called MNSTREM, based on a finite difference solution of the
nonlinear equation to predict SWT at one-hour increments for the Clearwater River (Sinokrot & Stefan, 1993). Similarly,
academic scientists in Canada introduced CEQUEAU, a water-balance type model which incorporated vegetation and soil
115 characteristics to solve for SWT (St-Hilaire et al., 2000). Physically based models became commercially available in the
2000s, one example being the MIKE suite of models, which were created to solve the heat and advection-dispersion equation
to simulate both surface and subsurface water dynamics, created by the DHI consulting group (Jaber & Shukla, 2012; Loinaz
et al., 2013). In addition to the models mentioned, over a dozen more physically based models were created and used
between 1990 and present day (Dugdale et al., 2017). For a more detailed review of physically based SWT models, we refer
120 the reader to Dugdale et al. (2017).

2.3 Artificial Intelligence Models in SWT modeling

Initial discussion of artificial intelligence can be traced back to 1943, when McCulloch and Pitts presented a computer model that functioned like neural networks of the brain (McCulloch & Pitts, 1943). In 1958, R.M. Friedberg published "A Learning Machine: Part 1", in IBM's Journal of Research and Development, one of the first to describe the concept of "machine learning". Friedberg hypothesized that machines could be taught how to learn such that they developed the capability to improve their own performance to the point of completing tasks or meeting objectives (Friedberg, 1958). Sixty years later, ML has grown as a field of study in academia and as an area of great interest in society, the latter due in large part to the popularity of large language models (a type of machine learning that we will not discuss here), such as ChatGPT (OpenAI, Inc., 2024), Copilot (Microsoft, Inc., 2024) and Gemini (Google LLC, 2024). For this review, we differentiate between traditional ML and newer ML, where the former includes approaches that have been used for decades in hydrologic modeling, i.e., cluster analysis, support vector machine, and shallow neural networks. We define newer ML as those introduced in hydrologic modeling in the few years, such as the deep learning long-short term memory NNs, extreme learning machine, and ML hybridizations. The following sections provide an overview of ML types and learning techniques. Finally, we assume that readers have a very basic understanding of the differences between machine learning types such as: supervised, semi-supervised, and unsupervised learning, and refer the reader to Xu and Liang (2021) for a nice overview.

2.3.1 Traditional ML algorithms

K-nearest neighbours (K-nn) is a type of supervised ML algorithm used to solve nonparametric classification and regression problems. It is one of the oldest algorithms (Fix & Hodges, 1952; Cover & Hart, 1967) considered within classical ML. The K-nn algorithm uses proximity between data points to make classifications or evaluations about the grouping of any given data point. While less used today, St. Hilaire (2012) used various K-nn model configurations to model SWT for the Moisie River in northern Quebec, Canada. The best K-nn model required prior-day SWT data and day-of-year (DOY), an indicator of seasonality (St-Hilaire et al., 2011). For five stream stations in Poland, Heddam et al. (2022) compare K-nn with other ML algorithms, finding that K-nn performed poorly compared to other ML algorithms.

Cluster analysis is a category of unsupervised ML methods used to create groups from an unlabeled dataset. Clustering methods use distance functions such as Euclidean distance, Manhattan distance, Minkowski distance, Cosine similarity and others, to group data into clusters (Irani et al., 2016). The analysis separates data into groups of maximum similarity, while also trying to minimize the similarity from group to group (Xu & Liang, 2021). In SWT modeling, studies have used cluster analysis to try a reduction of a dataset prior to assessment (Voza & Vuković, 2018) and/or to find spatiotemporal patterns in a dataset (Krishnaraj & Deka, 2020). Another popular clustering technique is discriminant analysis, which tries to find parameters that are most significant for temporal differentiation between rendered periods (Voza & Vuković, 2018). *K-means*, a type of unsupervised ML, is a clustering algorithm that finds 'k' number of centroids in the dataset and distributes each respective data value to the nearest cluster while keeping the smallest number of centroids possible (Krishnaraj & Deka,

2020). While cluster analysis and discriminant analysis are generally used to reduce datasets, another technique, the *Principal Component Analysis/factor test (PCA)*, is applied to assess dominant factors in datasets. Mathematically, Principal

155 Component Analysis (PCA) is a statistical unsupervised ML technique that uses an orthogonal transformation (a linear transformation that preserves lengths of vectors and angles) to convert a set of variables from correlated to uncorrelated (Krishnaraj & Deka, 2020). Krishnaraj and Deka (2020) used K-means and PCA in the Ganga River Basin of India to find spatiotemporal patterns of water quality parameters, including SWT.

Support vector machine (SVM) is a supervised learning technique used for classification, regression and outlier detection.

160 The aim of SVM is to find a hyperplane (or the decision surface) in an N-dimensional space (N = number of features) that best separates labeled categories, or support vectors (Cortes & Vapnik, 1995). One of the advantages of SVM is that it seeks to minimize the upper bound of the generalization error, instead of the training error (Cortes & Vapnik, 1995). A big disadvantage is that it does not perform well with large data sets due to the likelihood of greater noise, which would cause support vectors to overlap, making classification difficult. For a more detailed explanation of SVM, we refer the reader to

165 Cortes & Vapnik (1995) and Xu and Liang (2021). In the last few decades, SVM has been coupled with other ML models to find the best performing models for short-term water quality predictions (Lu & Ma, 2020) and daily SWT modeling (Heddam, Ptak, et al., 2022). For example, Heddam (2022), used *Least Squares SVM (LSSVM)*, a variant of SVM which takes a linear approach (instead of quadratic like SVM) to reach a solution (Suykens & Vandewalle, 1999). A version of SVM used for regression tasks is the *support vector regression (SVR)*. SVR attempts to minimize the objective function

170 (composed of loss greater than a specified threshold) and a regularization term (Rehana, 2019; Hani et al., 2023). For further detail on SVR, we refer the reader to Rehana (2019) and Hani et al., (2023). Using historical data, SVR has been compared with other ML models that evaluate SWT variability due to climate change (Rehana, 2019), finding temperature increases less pronounced in the SVR model. Jiang et al. (2022) compared SVR to other ML models to forecast SWT in cascade reservoir-influenced rivers. For the cascade reservoir operation-influenced study, SVR was outperformed by random forest

175 (RF) and gradient boosting (Jiang et al., 2022). Focusing on 78 catchments in the Mid-Atlantic and Pacific Northwest hydrologic regions of the U.S., researchers used SVR, and a ML algorithm called XGBoost to predict monthly SWT (Weierbach et al., 2022), finding that SVR significantly outperformed traditional statistical approaches such as multi-linear regression (MLR), but did not outperform XGBoost. In addition, the SVR models had the highest accuracy for SWT across different catchments (Weierbach et al., 2022). In Quebec, Canada, a comparison 4 ML models that estimated hourly SWT,

180 showed SVR outperformed by RF (Hani et al., 2023). A lesser-known form of SVM is its extended form, called *relevance vector machine (RVM)*. RVM is a form of supervised learning that uses a Bayesian framework to solve classification and regression problems (Tipping, 2001). *Locally weighted polynomials regression (LWPR)* is a form of supervised ML(Moore et al., 1997), used for learning continuous non-linear mappings from real-valued (i.e., functions whose values are real numbers) inputs and real-valued outputs. LWPR works by adapting the model locally to the respective data points, assigning

185 different weights to different data points based on data point proximity to the target (Moore et al., 1997). This type of

regression is best employed when the variance around the regression line is not constant, thereby suggesting heteroscedasticity.

Gaussian Process Regression (GPR) is a type of nonparametric supervised learning method used to solve regression problems. As a Bayesian approach, GPR assumes a probability distribution over all functions that fit the data. GPR is specified by a mean function and covariance kernel function which reflect prior knowledge of the trend and level of smoothness of the target function (Xu & Liang, 2021). One of GPR's advantages is the model's ability to calculate empirical confidence intervals, allowing the user to consider refitting predictions to areas of interest in the function space (Grbić et al., 2013). For more details on GPR, we refer the reader to Xu & Liang (2021). Grbic et al. (2013) used GPR for SWT modeling of the river Drava, Croatia. The authors created a predictive model consisting of two GPR models, where model #1 estimated the seasonal component of SWT fluctuations and model #2 estimated the shorter-term component (Grbić et al., 2013). A separate study for the river Drava used three variations of GPR to model SWT, finding that GPR was outperformed by the physically based, stochastically calibrated model, air2stream (Zhu, Nyarko, Hadzima-Nyarko, Heddam, et al., 2019). More recently, Majerska et al. (2024) used GPR to simulate SWT for a non-glaciated arctic catchment, Fuglebekken (Spitsbergen, Svalbard). Using GPR and another model, the authors identified a diurnal warming trend of 0.5-3.5 °C per decade through the summer season, implying a warming thermal regime in the Fuglebekken catchment (Majerska et al., 2024).

Decision trees (DTs) are a non-parametric, supervised learning technique. DTs can make predictions or decisions based on a set of input features and are likely to be more accurate where the problem can be solved in a hierarchical sequence of decisions (Breiman, 2001). *Classification and Regression Trees (CART)* is a specific type of algorithm that builds decision trees, where the internal node in the tree splits the data into two branches (sub-nodes) based on the specified decision rule (Loh, 2008). While CART can quickly find relationships between data, it is prone to overfitting and can be statistical unstable, where a small perturbation in the training data could negatively affect the output of the tree (Hastie et al., 2001; Xu & Liang, 2021). For a detailed explanation of DT and CART, we refer the reader to Hastie et al. (2001), Loh (2008) and Xu and Liang (2021). In the case of daily SWT modeling and prediction, DTs can perform similarly to GPR and NNs (Zhu, Nyarko, Hadzima-Nyarko, Heddam, et al., 2019). However, when comparing daily SWT results from DTs with Gradient Boosting (GB) or Random Forest (RF), DTs generally underperform (Anmala & Turuganti, 2021; Jiang et al., 2022). Recent studies have compared CART with other MLalgorithms to model water quality parameters (including SWT), finding that CART underperformed due to overfitting, compared to RF (Souaissi et al., 2023) and extreme learning machine, ELM (Heddam, Kim, et al., 2022). To combat the problem of overfitting that can occur using decision trees, the idea of using multiple trees by bootstrap aggregation (i.e., bagging), has gained interest. With *random forests (RF)*, a large number of individual decision trees work together as an ensemble (Breiman, 2001). Thus, an RF consists of multiple CARTs that stem from a bootstrap sample of the training data. Each individual tree in the random forest provides a class prediction and the class with the most votes (from the decision trees), becomes the model's prediction or the regression equivalent (Breiman, 2001). While RF is considered less interpretable than individual decision trees, RF can calculate importance scores from input variables which provide information about dominant factors influencing the target variable (Xu & Liang, 2021). Other

220 tree ensemble algorithms used in SWT modeling include XGBoost (Lu & Ma, 2020) and gradient/adaptive boosting machine (Jiang et al., 2022). In 2020, a study used RF and XGBoost to predict six water quality indicators (including SWT) at hourly time steps for a river in Oregon (Lu & Ma, 2020). Researchers found that an advanced data denoising technique called *complete ensemble empirical mode decomposition with adaptive noise (CEEMDAN)*, improved model performance for both RF and XGBoost. For more information on CEEMDAN, we refer the reader to Lu and Ma (2020). Like Lu and Ma (2020),

225 Feigl et al. (2021) tested the performance of six ML models, including RF and XGBoost, for daily SWT prediction in 10 Austrian catchments. Results showed minor difference in model performance, with a median RMSE difference of 0.08 °C between tested ML models (Feigl et al., 2021). Jiang et al. (2022) tested the performance of six ML models in estimating daily SWT below dams in China. They found that day of year was most influential for the prediction of SWT, followed by stream flow flux and AT (Jiang et al., 2022). Weierbach et al. (2022) used XGBoost and SVR to predict SWT at monthly

230 time scales, finding that an ensemble XGBoost outperformed all modeling configurations for spatiotemporal predictions in unmonitored basins. In contrast to Jiang et al. (2022), Weierbach et al. (2022) found AT as the primary driver of monthly SWT for all 78 sites in the Pacific Northwest region of the U.S. (which included areas affected by dams), followed by month of year and solar radiation. Zanoni et al. (2022) used RF and a deep learning model to develop regional models of SWT and other water quality parameters, finding that RF performance was less effective at detecting non-linear relationships than to

235 the deep learning model. They found AT to be most influential, with day of the year, and year of observation as possible replacements where AT was not available (Zanoni et al., 2022).

Souassi et al. (2023) tested the performance of two ML models, RF and XGBoost, with non-parametric models for the regional estimation of maximum SWT at ungaged locations in Switzerland, finding no significant differences between the ML performance and the non-parametric model performances, which was attributed to the lack of a large dataset as required

240 by the ML models. Hani et al. (2023) used four supervised ML models – MARS, GAM, SVM, and RF to model potential thermal refuge area (PTRA) at an hourly timestep for two tributary confluences of the Sainte-Marguerite River in Canada. RF had the highest accuracy at both locations in terms of hourly PTRA estimates and modeling SWT (Hani et al., 2023). Wade et al. (2023) conducted a CONUS-scale study using 410 USGS sites with four years of daily SWT and discharge to examine maximum SWT. They used RF to estimate max SWT and thermal sensitivity (Wade et al., 2023), finding that AT

245 was the most influential control followed by other properties (watershed characteristics, hydrology, anthropogenic impact). The *Least Absolute Shrinkage and Selection Operator (LASSO)* is a regression technique used by researchers interested in selecting predictor variables (Tibshirani, 1996). Research considering ML models for SWT frequency analysis at ungaged basins used the LASSO method to select explanatory variables for two ML models (Souaissi et al., 2023). The LASSO method consists of a shrinkage process where the method penalizes coefficients of regression variables by minimizing them

250 to zero (Tibshirani, 1996). The number of coefficients set to zero depends on the adjustment parameter, which controls the severity of the penalty. Thus, the method can perform both feature selection and parameter estimation, an advantage when examining large datasets (Xu & Liang, 2021).

2.3.2   Traditional artificial neural networks (ANN)

The first study that utilized artificial neural networks specifically for SWT modeling was published around the year 2000.
255   The work was done by researchers interested in hindcasting SWT for a river in Canada, for a 41-year period dating back to 1953 (Foreman et al., 2000). Since 2000, various types of artificial neural networks have been increasingly used to model SWT at various sites at hourly, daily and monthly time steps. The following sections describe the use of NNs for SWT modeling. An *artificial neural network (ANN)* is a type of ML algorithm inspired by biological NNs in the brain (McCulloch & Pitts, 1943; Hinton, 1992). ANNs learn from data provided and improve on their own to progressively extricate higher-
260   level trends or relationships within the given dataset (Hinton, 1992). Currently, ANNs are capable of data classification, pattern recognition, and regression analysis. Considered robust, ANNs can undergo supervised, unsupervised, semi-supervised and reinforcement learning.

ANNs are composed of networks of interconnected neurons, also called nodes or units. The network architecture of a commonly used ANN, the *feed-forward NN (FFNN)*, can be described as a three- (or more) layered network of connected
265   neurons, organized from left-to-right, where the input layer is the first layer, the centre layer (could be one or more) is "hidden", and the last layer is the output layer (Risley et al., 2003). *Multi-layer perceptron NNs (MLPNN)* fall under the umbrella of FFNNs. In the FFNN architecture, the first (left-most) layer creates input signals from a dataset. In the hidden layer, the neurons process the input signals using an activation function (i.e., step, sigmoid-shaped, hyperbolic tangent, etc.), to calculate a hidden-layer output from the input, the hidden-layer weight, and the hidden-layer bias (Hinton, 1992). The
270   hidden-layer weight is defined as the strength of the influence of neurons on each other and is modifiable (Hinton, 1992). For example, a connection between neurons A and B may be stronger (weight ~0.5) than a connection between neurons B and C (weight ~0.1). This weight can be adjusted, or "fine-tuned" to minimize errors. Depending on the output of the activation function, the output signals may be transmitted to other neurons in the network, eventually supplying output from the hidden layer to the final layer, which computes the final output using a summation function (Hinton, 1992).

275   The backpropagation (BP) learning algorithm (Hinton, 1992) is one of the more popular techniques that iteratively adjusts model weights and bias terms in a neural network. First, the FFNN is trained on a labelled/categorized dataset, called the "training" dataset. The BP algorithm then iteratively adjusts weights in the NN based on the calculated error between the predicted output and the actual output, allowing the NN to find underlying patterns or possible relationships in the data (Hinton, 1992). However, use of the BP learning algorithm for FFNNs can be time-consuming in terms of training and
280   calibration (Huang et al., 2006). Huang et al. (2006) proposed an alternative learning algorithm called *extreme learning machine (ELM)* for shallow-layer BP FFNNs (also abbreviated to BPNNs). The ELM algorithm optimizes training by randomly choosing hidden nodes and analytically finding output weights (Huang et al., 2006). In a comparison study, ELM generally outperformed the BP algorithm in terms of learning and performance (Huang et al., 2006).

Another kind of ANN with a similar three-layer structure is the *radial basis function NN (RBFNN)*. However, the RBFNN
285   distinction is that only one hidden layer is used and that the width of connections and centres (distance between inputs and

weights) must be calculated prior to adjusting weights (Musavi et al., 1992; Buhmann, 2000). We refer the reader to Musavi et al. (1992) and Buhmann (2000) for more detail on RBFNN. The *Cascade Correlation Neural Network (CCNN)*, introduced by Fahlman and Lebiere (1989), proved to be much faster than back-propagation (Fahlman & Lebiere, 1989). The CCNN was created with a cascade architecture, where hidden neurons are added to the network one at a time and remain

290   unchanged, i.e., the input weights are frozen, allowing the neuron to become a feature-detector in the network, capable of either producing outputs or creating other, complex feature detectors (Fahman and Lebiere, 1989). For more detail on CCNN, we refer the reader to Fahman and Lebiere, 1989.

General Regression NN, is a Bayesian type of FFNN based on kernel regression networks (Specht, 1991). Unlike MLPNN, GRNN does not need an iterative training procedure like backpropagation. One of the advantages of GRNN with

295   increasingly larger datasets is that it is consistent in forcing the estimation error to approach zero with only minor restrictions on the function (Specht, 1991). GRNN also differs from RBFNN in the method used to decide the weights of the hidden layer nodes. GRNN does not train the weights as RBFNN does, instead, GRNN provides the target value (to the node weight) by considering the input training data set and the related output (Specht, 1991). The *Product-Unit NN (PUNN)*, uses product units (in contrast to the summation units used by MLPNN), to compute the product of its inputs, each raised to a

300   variable power (Janson & Frenzel, 1993). While less used in SWT modeling, PUNNs have garnered interest due to their capacity for implementing higher order functions (Martínez-Estudillo et al., 2006), and advantage of requiring less parameters for optimization, when considering the same number of input nodes, hidden nodes, and output nodes (Piotrowski et al., 2015). For more on PUNN, we refer the reader to Janson and Frenzel (1993) and Martínez-Estudillo et al. (2006). A lesser known but used neural network is the *Group Method of Data Handling (GMDH)*, created by Russian scientist

305   Ivakhnenko in the late 1960s for the purpose of using inductive learning methods for modeling complex, non-linear systems without the bias of the user (Ivakhnenko, 1970). Although not initially described as a NN, GMDH is a polynomial NN. GMDH initiates only with input neurons, then during the training processes, neurons are "self-organized" to optimize the network with the help of "control data" to stop the training process when overfitting occurs (Ivakhnenko & Ivakhnenko, 1995; Graf & Aghelpour, 2021). For more information on GMDH, we refer the reader to Ivakhnenko (1970) and Ivakhnenko

310   & Ivakhnenko (1995).

Adaptive-network-based fuzzy inference systems (ANFIS) are a type of NN using fuzzy inference, initially proposed by Jang (1993). Fuzzy inference systems first interpret values in the input vector, then (following a set of rules), the system assigns values to the output vector (Kalogirou, 2023). ANFIS uses a combination of fuzzy inference, and adaptive network learning (a superset of all FFNNs) to make and improve upon its estimations (Jang, 1993). In SWT modeling, ANFIS has been

315   included in comparisons with other NNs for model performance evaluation (Piotrowski et al., 2015; Zhu, Heddam, Nyarko, et al., 2019; Zhu, Hadzima-Nyarko, Gao, Wang, et al., 2019; Graf & Aghelpour, 2021). A different type of fuzzy NN is the *dynamic neuro-fuzzy local modeling system (DNFLMS)*, which contrasts with ANFIS by its use of the one-pass clustering algorithm and sequential learning algorithm (Hong & Bhamidimarri, 2012). A comparison of ANFIS and DNFLMS showed

that the latter requires less training in terms of fuzzy rules needed and less epochs, which can result in over 18.5 hours saved
320   in computing time (Hong & Bhamidimarri, 2012).

2.3.3   Newer/recent ML algorithms

We define newer/recent ML algorithms as those introduced or re-introduced in the last decade for SWT modeling. These ML algorithms include deep (i.e., increased layers) ANNs such as recurrent neural networks (RNN), convolutional neural networks (CNN), extreme learning machine (ELM), ML hybridizations and subsets.

325   A *"deep" neural network (DNN)* has three or more hidden layers, MLPNNs being one such example. The purpose of added layers is to serve as optimizations for greater accuracy. Due to their complex nature, DNNs need extensive time spent solely on training the network on the input data (Abdi et al., 2021). *Convolutional neural networks (CNN)* are FFNNs used to recognize objects and patterns in visual data (LeCun et al., 1989, 2004). CNNs have convolutional layers, which hold one or more filters that calculate a local weighted sum as they analyse the input data. A CNN filter is a matrix (rows and columns)
330   of randomized number values that convolves (i.e., moves), through the pixels of an image, taking the dot product of the matrix of values in the filter and the pixel values of the image. The dot product is used as input for the next convolutional layer. To ensure adequate performance, CNNs must be trained with examples of correct output in the form of labelled training data and should be calibrated (i.e., adjusting filters, implement loss functions) to optimize performance (Krizhevsky et al., 2012). For more detail on CNN, we refer the reader to LeCun et al. (2004), Krizhevsky et al., (2012) and Xu and Liang
335   (2021). A disadvantage of CNNs is that they are not ideal for interpreting temporal or sequential information or data that require learning from past data to predict future output. For interpreting temporal information or sequential data, recurrent neural networks are preferred.

Unlike FFNNs, recurrent neural networks (RNN) work in a chain-link nature that allows them to loop (i.e., keep) previously handled data for use in a present task to make better predictions (Hochreiter & Schmidhuber, 1997). The RNN architecture is
340   better equipped (and preferred) to handle temporal (i.e., time series) or sequential (i.e., a video is a sequence of images) data due to their ability to learn from their past (Bengio et al., 1994). The *Elman neural network (ELM-NN)* is a type of RNN where the hidden layer (bi-directionally connected to the input layer and output layer) stores contextual information of the input that it sends back to the input layer with sequential time steps (Elman, 1990).

However, one of the issues that persists in RNNs, is that there is a limit to how far back RNNs can access past data to make
345   better predictions. This is described as the problem of long-term dependencies, also known as the vanishing gradient problem. The vanishing gradient problem is due to backpropagated gradients that can grow or shrink at each time step, increasing instability until the gradients "explode" or "vanish" (Bengio et al., 1994; Hochreiter & Schmidhuber, 1997). Hochreiter & Schmidhuber (1997) introduced the *long-short term memory (LSTM)* model, a type of RNN explicitly designed to overcome the vanishing gradient problem. The LSTM architecture includes three gates (input, forget, and output gates)
350   that control the flow of information in and out of the cell state, allowing the NN to store and access data over longer time periods. In the last few decades, LSTMs have improved, and variations introduced (Gers & Schmidhuber, 2000; Cho et al.,

2014; Yao et al., 2015) and many have been cross compared, with findings showing similar performance across LSTMs (Greff et al., 2016). In the last few years, LSTMs and their variations have been revisited and employed in hydrologic studies to examine possible relationships in time series data (Shi et al., 2015; Shen, 2018; Kratzert et al., 2018, 2019). For example,

355 Sadler et al. (2022) used a LSTM model to multi-task, i.e., predict two related variables – streamflow and SWT. Their argument for forcing a LSTM to multi-task is that if two variables are driven by the same underlying physical processes, a multi-tasking LSTM could more wholistically represent shared hydrologic processes and thus better predict the variable of interest. Their LSTM model consisting of added components: specifically, two parallel, connected output layers that represented streamflow output and SWT output (Sadler et al., 2022). Overall, using the multi-tasking LSTM improved

360 accuracy for half the sites, but for those sites with marked improvement, more calibration was needed to reach improvement (Sadler et al., 2022).

Another type of NN is the *graph neural network (GNN),* which is used for representation learning (unsupervised learning of feature patterns) of graphed data, where a "graph" denotes the links between a collection of nodes. At each graph node or link, information in the form of scalars or embeddings can be stored, making them very flexible data structures. Example of

365 graphs that we interact with regularly are images, where each pixel is a node and is linked to adjacent pixels. A stream network is also an example of a graph, albeit a directed graph, which is a graph in which the links (also called 'edges') have direction. Two examples of recent GNNs are *recurrent graph convolution networks (RGCN)* and *temporal convolution graph models (TCGM).* The RGCN utilizes LSTM network architecture (i.e., use of forget, input, output gates) for temporal recognition (Topp et al., 2023). In contrast to RGCN, TCGM uses 1D convolutions (i.e., input a 3-dimensional object and

370 output a 3-dimensional object), pooling, and channel-wise normalization to capture low-, intermediate- and high-level temporal information in a hierarchical manner (Lea et al., 2016). An example that utilizes this approach is Graph Wave Net (Wu et al., 2019), which has been used in spatial-temporal modeling of SWT (Topp et al., 2023). According to Topp et al. (2023), the temporal convolutional structure of Graph Wave Net is more stable in the gradient-based optimization process in contrast to the possible gradient explosion problem that the LSTM in the RGCN could experience.

375 While present studies continue to use ML models as standalones to evaluate SWT predictions, other studies have coupled modern ML with non-ML models to examine whether such combinations improve model performance (Graf et al., 2019; Qiu et al., 2020; Rehana & Rajesh, 2023). For example, Graf et al. (2019) coupled four discrete wavelet transform (WT) techniques with MLPNN to predict SWT for eight stations on the Warta River in Poland. For reference, WT is widely applied for the analysis and denoising of information (signals) and images both over time and on a domain scale (frequency).

380 The unique characteristic of a WNN is the use of the WT as the activation function in the hidden layer of the NN (Qiu et al., 2020). Zhu, Hadzima-Nyarko, Gao et al. (2019) coupled WT with MLPNN and ANFIS to evaluate daily SWT at two stations on the River Drava in Croatia, and separately compared the WT-ML coupling with MLR. The study found that the combination of WT and ML improved performance compared to the standalone models (Zhu, Hadzima-Nyarko, Gao, Wang, et al., 2019).

385 A recent ML approach called differentiable modeling, incorporates physics into ML modeling frameworks, where the basic model structure and parameters of a process-based model are inserted into an ANN to estimate parameters or replace existing process descriptions (Rahmani et al., 2023). Rahmani et al. (2023) examined model components that could improve a LSTM model's ability to better match model predictions to field observations. From their study, Rahmani et al. (2023) found that adding a separate shallow subsurface flow component to the LSTM model, and a recency-weighted averaging of past AT for
390 calculating source SWT resulted in improved predictions (Rahmani et al., 2023).

2.4 SWT predictions using ML

2.4.1 Local: Single rivers, Site-specific (≤ 100 km^2)

SWT predictions using ML have extended from the local scale to nearly continental scales over the last 24 years. One of the first studies to use a neural network to estimate SWT used a MLPNN was done by Sivri et al., (2007) who predicted monthly
395 SWT for Firtina Creek in Türkiye, a novel approach at the time. While the MLPNN model R^2 ~ 0.78 was not very good, the proof of concept was a success (Sivri et al., 2007). Chenard and Caissie (2008) used eight ANNs to calculate daily and max SWT for Catamaran Brook, a small drainage basin tributary to the Miramichi River in New Brunswick, Canada for the years 1992 to 1999. Their ANN models performed best in late summer and autumn and performed comparatively to stochastic models for the same watershed (Chenard & Caissie, 2008). In 2009, Sahoo et al. (2009) compared a NN, multiple regression
400 analysis, and dynamic non-linear chaotic algorithms (Islam & Sivakumar, 2002) to estimate SWT in the Lake Tahoe watershed area in along the California/Nevada border within the U.S. Their NN models included available solar radiation and AT, with results showing a variation of the BPNN as having the best performance (Sahoo et al., 2009).

Hadzima-Nyarko et al. (2014) used a linear regression model, a stochastic model, and variations of two NNs: MLP (six variations) and RBF (two variations), to compute and compare SWT predictions for four stations on the river Drava, along
405 the Croatia-Hungary border in southern Central Europe. While their ANN models performed better than the linear regression and stochastic models, a comparison of their NN models found that one of their six MLPNN variations barely outperformed the RBFNN, with a difference in RMSE of 0.0126 °C, within the margin of error. The authors stated that apart from the current mean AT, the daily mean AT of the prior two days and classification of the day of the year (DOY) were significant controls of the daily SWT (Hadzima-Nyarko et al., 2014). Rabi et al. (2015) conducted a study using the same gage stations
410 on the river Drava using only AT as a predictor and restricted the use of NNs to only MLP, finding that the MLPNN outperformed the linear regression approaches (Rabi et al., 2015).

Cole et al. (2014) tested a suite of models including an FFNN to predict SWT downstream of two reservoirs in the Upper Delaware River, in Delaware, U.S. During training, the FFNN was outperformed by an Auto Regressive Integrated Moving Average (ARIMA) model and performed similarly to the physically based Heat Flux Model, HFM (Cole et al., 2014).
415 During testing, the FFNN, ARIMA, and HFM models performed similarly, with HFM being slightly more accurate due to its advantage as a physically based model with data availability and calibration potential (Cole et al., 2014). The authors suggest

that the under/over-predictions of the models may have been from unaddressed groundwater inputs or unaccounted for nonlinear relationships (Cole et al., 2014). Hebert et al. (2014) focused on the Catamaran Brook area (like Chenard and Caissie, 2008) and included the Little Southwest Miramichi River in New Brunswick, Canada, to conduct ANN model
420 predictions of hourly SWT. The study considered spring through autumn, hourly data from 1998 to 2007, finding that the ANN models performed similarly or better than deterministic and stochastic models for both areas (Hebert et al., 2014). Piotrowski et al. (2015) examined data from two streams, one mountainous and one lowland, in a moderately cold climate of eastern Poland, to model SWT using MLPNN, PUNN, ANFIS, and WNN. The ANN models were independently calibrated to find the best fits, with results showing that MLPNN and PUNN slightly outperformed ANFIS and WNN (Piotrowski et
425 al., 2015). The study also found current AT, and information on the mean, maximum, and minimum AT from 1-2 days prior as important for improving model accuracy (Piotrowski et al., 2015). Temizyurek and Dadaser-Celik (2018) used an ANN with observations of AT, relative humidity, prior month SWT and wind speed to predict monthly SWT at four gages on the Kızılırmak River in Turkey. Best results were obtained from using the sigmoidal (S-shape) activation function and the scaled conjugate gradient algorithm (Møller, 1993), though the average RMSE (~2.3 °C) for the NN used was higher (worse) than
430 the average calculated from this literature review where RMSE ~1.4° C.

Zhu et al. (2019) conducted four studies that used NNs to examine SWT on the river Drava, Croatia (Zhu, Hadzima-Nyarko, Gao, Wang, et al., 2019; Zhu, Heddam, Nyarko, et al., 2019; Zhu, Nyarko, Hadzima-Nyarko, Heddam, et al., 2019). They also examined SWT of three rivers in Switzerland (Zhu, Heddam, Nyarko, et al., 2019; Zhu, Nyarko, Hadzima-Nyarko, Heddam, et al., 2019), and three rivers in the U.S. (Zhu, Heddam, Wu, et al., 2019; Zhu, Nyarko, Hadzima-Nyarko, Heddam,
435 et al., 2019). Across the studies, the MLPNN models had better performance compared to ANFIS (Zhu, Heddam, Nyarko, et al., 2019), GPR (Zhu, Nyarko, Hadzima-Nyarko, Heddam, et al., 2019), or MLR (Zhu, Heddam, Wu, et al., 2019). Qiu et al. (2020) used variations of NNs (MLP/BPNN, RBFNN, WNN, GRNN, ELMNN) to examine SWT at two stations on the Yangtze River, China, finding that the MLP/BPNN outperformed all other models when the particle swarm algorithm (PSO) was used for optimization (Qiu et al., 2020). Stream discharge and DOY were also shown to improve model accuracy.
440 Piotrowski et al. (2020) used various MLPNN shallow (1 hidden layer) structures to test the use of an approach called dropout in SWT modeling using data from six stations in Poland, Switzerland, and the U.S. The dropout approach can be applied to deep ANNs due to its efficiency in preventing overfitting and low computation requirements (Piotrowski et al., 2020). The study found that use of dropout and drop-connect significantly improved performance of the worst training cases. For more information on the use of dropout with shallow ANNs, we refer the reader to Piotrowski et al. (2020).

445 Graf and Aghelpour (2021) compared stochastic and ANN (ANFIS, RBF, GMDH) SWT models for four gages on the Warta River, in Poland, finding that all models performed similarly well (R^2 > 97.6 %). Results showed that the stochastic and ML models performed similarly, while the stochastic models had less prediction errors for extreme SWT (Graf & Aghelpour, 2021). Rajesh and Rehana (2021) used several ML models (Ridge regression, K-nn, RF, SVR) to predict SWT at daily, monthly and seasonal scales for a tropical river system of India. The authors found that the monthly SWT prediction performed better than the daily or seasonal (Rajesh and Rehana, 2021). Of the ML models, the SVR was the most robust,
450

though a data assimilation algorithm notable improved predictions (Rajesh and Rehana, 2021). Jiang et al. (2022) examined SWT under the effects of the Jinsha River cascaded reservoirs using six ML models (i.e., adaptive boosting, AB, decision tree, DT, random forest, RF, support vector regression, SVR, gradient boosting, GB, and multilayer perceptron neural network, MLPNN). The study found that day of year (DOY) was most influential in each model for SWT prediction,

455   followed by stream flow and AT (Jiang et al., 2022). With knowledge of the influential parameters, ML model variations were tested, finding that gradient boosting and random forest provided the most accurate estimation for the training dataset and the test dataset (Jiang et al., 2022). Abdi et al. (2021) used linear regression and a deep (multi-layered) neural network (DNN) to predict hourly SWT for the Los Angeles River, finding that the DNN outperformed the linear regressions. They suggested that using a variety of ML models to predict SWT could add robustness to a study, but state that training ANNs is

460   more time-consuming than training linear regression models, for minimal improved accuracy (Abdi et al., 2021). Khosravi et al. (2023) used an Exploratory Data Analysis (EDA) technique, a type of feature engineering that prepares the dataset for best performance with an LSTM to identify SWT predictors (discharge, water level, AT, etc.) up to one week in advance for a monitoring station on the Central Delaware River. The authors noted that though the LSTM performed satisfactorily, future studies should compare LSTMs with CNNs or other model types, and that generalizability is limited to the specific location

465   and dataset (Khosravi et al., 2023). Majerska et al. (2024) used GPR to simulate SWT for the years 2005-2022 for the artic catchment Fuglebekken in Svalbard, Norway. The unique opportunity to study SWT of an unglaciated High Arctic stream regime showed an alarming warming throughout the summer where SWT increased as much as 6 °C, highlighting a strong sensitivity of the Arctic system to ongoing climate change (Majerska et al., 2024).

2.4.2 Regional, Continental Scale (≥ 100 km^2)

470   DeWeber and Wagner (2014) conducted one of the first regional ANN ensemble studies, focusing on thousands of individual streams reaches across the Eastern U.S. They used an ensemble of 100 ANNs to estimate daily SWT with varying predictors for the 1980 – 2009 period, finding that daily AT, prior 7-day mean AT and catchment area were the most important predictors (DeWeber & Wagner, 2014). In Serbia, Voza and Vukovic (2018) conducted cluster analysis, PCA and discriminant analysis for the Morava River Basin using data from 14 river stations to identify monitoring periods for

475   sampling. With discriminant parameters identified, an MLPNN was used to predict changes in the values of the discriminant factors (see fig. 1 of Voza and Vukovic, 2018) and identify controls on the monitoring periods, finding that seasonality and geophysical characteristics were most influential (Voza & Vuković, 2018).

Rahmani et al. (2021) used four years of SWT data for 118 sites across the CONUS to test three LSTM models that simulated SWT, finding that the LSTM trained with streamflow observations was the most accurate, which was

480   unsurprising. Of interest to the reader would be the inner mechanisms of the LSTM, but the study could not explicitly state what physical laws (if any) were followed by the LSTM. Instead, the authors hypothesized that the LSTM could assume internal representations of physical quantities (i.e., water depth, snowmelt, net heat flux, baseflow temperature, SWT). The authors further stated that the LSTM was dependent on a good historical data record and would not generalize well to

ungauged basins. Feigl et al. (2021) tested the performance of six ML models: stepwise linear regression, RF, XGBoost,

485 FFNNs, and two RNNs (LSTM and GRU) using data from 10 gages in the Austria-Germany-Switzerland region, to estimate daily SWT. From the comparison, FFNNs and XGBoost were the best performing in 8 of 10 catchments (Feigl et al., 2021). For modeling SWT in large catchments (> 96,000 km^2 ~ Danube catchment size), the RNNs performed best due to their long-term dependencies (Feigl et al., 2021). Zanoni et al. (2022) used RF, DNN, and a linear regression to predict daily SWT in the Warta River basin and compared the results with those of stochastic models. Their results found that the DNN was the

490 most effective in capturing nonlinear relationships between drivers (i.e., SWT) and water quality parameters (Zanoni et al., 2022). On parameter influence, the analysis also found that DOY was an adequate surrogate for AT input in modeling SWT, experiencing only a slight performance reduction.

Heddam, Ptak, et al., (2022) used six ML models: K-nn, LSSVM, GRNN, CCNN, RVM, and LWPR, to evaluate SWT for several of Poland's large rivers. For each ML, three variations were created: one calibrating with only AT as input, another

495 calibrating with AT and DOY, and a third decomposing AT using the variational mode decomposition, VMD (Heddam, Ptak, et al., 2022). For more on VMD, we refer the reader to Heddam, Ptak, et al., 2022a. The study found that the VMD parameters improved RMSE and MAE performance metrics for some models, but neither GRNN or K-nn showed improvement. Heddam, Kim, et al., (2022) examined how use of the Bat algorithm optimized the extreme learning machine (Bat-ELM) neural network and how that in turn affected modeling of SWT in the Orda River in Poland. Results from the

500 Bat-ELM were compared with MLPNN, CART, and multiple linear regression, MLR, finding the Bat-ELM outperformed MLPNN, CART and MLR (Heddam, Kim, et al., 2022). Focusing on a region of Germany, Drainas et al. (2023) trained and tested various ANNs with different inputs, for 16 small (≤1 m^3/s) headwater streams. They found that the best performing (lowest RMSE) input combination was stream-specific, suggesting that the optimal input combination cannot be generalized across streams for the region (Drainas et al., 2023). The ANN prediction accuracy of SWT was negatively affected by river

505 length, total catchment area and stream water level (Drainas et al., 2023). Additionally, ANN accuracy suffered when dealing with open-canopy land use types such as grasslands but improved with semi-natural and forested land cover (Drainas et al., 2023). Recently, He et al. (2024) built a LSTM framework to model water dynamics in stream segments while attempting to capture spatial and temporal dependencies. First, a baseline LSTM+GNN, then improved it by using graph masking and adjusting the model based on constraints (He et al., 2024). For the Delaware River Basin, the Fair-Graph model

510 performed slightly better than the baseline with a RMSE of 1.833 vs. 1.786, respectively. For the Houston River network, the Fair-Graph model also performed slightly better than the baseline (NSE of 0.721 vs. 0.580). While the relative performance compared to baseline was not significantly better, we anticipate that graph masking (algorithm that incorporates spatial awareness into ANN), will play an increasingly large role in hydrologic modeling (Shen, 2018; He et al., 2024).

2.5. Decision Support and Climate Change Scenarios

515 In 2003, the United States Geological Survey (USGS), used a FFNN to estimate hourly SWT for a summer season in western Oregon (Risley et al., 2003). Their work used the predicted SWT to better constrain future total maximum daily loads

(TMDL) for stream management. Jeong et al. (2016) used an ANN to evaluate SWT for the Soyang River, South Korea. The goal was to couple the ANN predictions with a cyber infrastructure prototype system to deliver automated, real-time predictions using weather forecast data (Jeong et al., 2016).

520 Liu et al. (2018) used a hydrological model called the Variable Infiltration Capacity (VIC) model to produce estimates of AT and river section-based variables for the Eel River Basin, Oregon, U.S., to be used as input data for an ANN. The study considered the AT rise from the RCP 8.5 scenario to estimate future (2093–2100) daily stream flow and SWT, finding that SWT was increasingly sensitive to the proportion of base flow in the summer (Liu et al., 2018). Topp et al. (2023) used the Delaware River Basin in the eastern U.S. to compare two DL models: a recurrent graph convolution network (RGCN), and a
525 temporal convolution graph model, TCGM, called Graph Wave Net. The comparison included scenarios capturing climate shifts representative of long-term projections where warm conditions or drought persisted. Considered spatiotemporally aware, the two process-guided deep learning models performed well (test RMSE of 1.64 °C and 1.65 °C); however, Graph WaveNet significantly outperformed RGCN in 4 of 5 experiments where test partitions represented diverse types of unobserved environmental conditions. Rehana and Rajesh (2023) used a standalone LSTM, a WT-LSTM, and a k-nearest
530 neighbour (K-nn) bootstrap resampling algorithm with LSTM, to assess climate change impacts on SWT using downscaled projections of AT with RCPs of 4.5 and 8.5 for seven polluted river catchments in India. Comparing the coupled models and the physically based air2stream model, they found the K-nn coupled with LSTM to be the best performing in terms of effectively predicting SWT at the monthly time scale. Considering the RCP scenarios, the predicted SWT increase for 2071–2100 for the rivers in India, ranged from 3.0–4.7 °C.

535 **3 Model Evaluation Metrics**

The second part of this review was to compile ML performance evaluation metrics as it pertains to SWT modeling and prediction and consider the commonly used metrics and suggest guidelines for easier comparison of ML performance across SWT studies. We considered journal articles from 2000–2024 that used ML to evaluate, predict, or forecast SWT and examine what model performance metrics had been used. Performance metrics can be calculated during model calibration,
540 testing, and (or) validation to compute a single value that denotes the agreeableness between simulated and observed data. For this literature review, all journals examined used least one metric to evaluate model performance, with two or more metrics used by > 84 % of studies published on or after the year 2019. For review, the quantitative statistics were split into three categories: standard regression, dimensionless and error index (Moriasi et al., 2007). Standard regression statistics are ideal for examining the strength of the linear relationship between model simulations/predictions and the observed/measured
545 data. Dimensionless techniques provide a relative assessment of model performance, but due to their interpretational difficulty (Legates & McCabe, 1999) have been less commonly used. In contrast, error indices quantify the error in terms of the units of the data (i.e., °C) considered.

3.1 Model Performance Metrics: Standard Regression

The most basic statistics (slope, y-intercept mean, median, standard deviation) continue to be use in part due to their
550   simplicity and ease of interpretability. These statistics are useful for preliminary examinations, where the assumption is that
measured and simulated values are linearly related, and all the variance of error is contained within the
predictions/simulations, whilst the observations are free of error. Unfortunately, observations are rarely error-free, and
datasets are nonlinear, highlighting a need for using a diverse set of statistics (Helsel and Hirsch, 2002). One such set of
statistics that are commonly used for standard regressions are called the correlation coefficients – Kendall's tau, Spearman's
555   rho, and Pearson's r. For this review, we focus on Pearson's r, which is a measure the linear association between two
variables of interest, typically observed and simulated data. Pearson's r is useful for determining the strength and direction
(i.e., positive, negative) of a linear relationship (Helsel and Hirsch, 2002). Values of r, range from -1 to +1, where $r < 0$
indicates a negative correlation and $r > 0$ indicates a positive correlation (Legates and McCabe, 1999). The square of r is
denoted as R^2, or the coefficient of determination, which represents the fraction of the variance in one variable (i.e.,
560   observations) that can be explained by the other variable (i.e., predictors). R^2 ranges from 0 to 1, with $R^2 = 1$ suggesting that
the model can explain all the variance, and vice versa. The r and R^2 metrics are typically used for normally distributed data
that follows a bivariate normal distribution (Helsel and Hirsch, 2002). In contrast to r and R^2, Spearman's rank correlation
coefficient, rho (ρ) is a non-parametric rank-sum test useful for analysing non-normally distributed data and nonlinear
monotonic relationships (Helsel and Hirsch, 2002). The data is ranked on a range from -1 to +1, where $\rho = 0$ indicates no
565   association and $\rho = $ -1 or +1 suggest a perfect monotonic relationship. By ranking the data, Spearman's correlation
coefficient quantifies monotonic relationships between two variables (converts nonlinear monotonic relationships to linear
relationships) allowing ρ to be robust against outliers (Helsel and Hirsch, 2002).

3.2 Model Performance Metrics: Error Indices

The mean absolute error (MAE), mean square error (MSE) and root mean squared error (RMSE) are popular error
570   indices used to assess model performance. The equations for MAE, MSE, and RMSE are:

$$MAE = \frac{1}{N}\sum_{i=1}^{N}|O_i - P_i| \qquad\qquad \text{eq. 1}$$

$$MSE = \frac{1}{N}\sum_{i=1}^{N}(P_i - O_i)^2 \qquad\qquad \text{eq. 2}$$

575

$$RMSE = \sqrt{\frac{\sum_{i=1}^{N}(P_i - O_i)^2}{N}} \qquad\qquad \text{eq. 3}$$

For the equations, N is the number of samples, O_i is the observed SWT and P_i is the predicted SWT at time, i. The
MAE computes the average magnitude of the errors in a set of predicted values to obtain the average absolute difference

between the predicted, P_i and the observed, O_i. In contrast to MAE, the MSE squares the error terms, resulting in the squared

580 average difference between the predicted and observed values. The resultant MSE is not in the same units as the value of

interest making it difficult to interpret. As the square root of the MSE, RMSE provides an error index in the unit of the data

(Legates and McCabe, 1999). However, both the MSE and RMSE are more sensitive to outliers and less robust than MAE.

$$PBIAS = 100 \cdot \frac{\sum_{i=1}^{N}(P_i - O_i)}{\sum_{i=1}^{N} O_i} \qquad \text{eq. 4}$$

585

Another error index used in SWT modeling is called the percent bias (PBIAS) index. PBIAS computes the average

tendency of model predictions to be greater or smaller than the observations/measurements (Gupta et al., 1999). A PBIAS

value of 0 is best, and low-magnitude values (closer to 0), denote stronger model accuracy. Positive PBIAS values suggest

model underestimation, while negative PBIAS values suggest model overestimation (Moriasi et al., 2007).

3.3 Model Performance Metrics: Error Indices

590

The Nash-Sutcliffe Efficiency (NSE, also called NSC, NS, or NASH), is a "goodness-of-fit" criterion that describes the

predictive power of a model. Mathematically, the NSE is a normalized statistic that computes the relative magnitude of the

variance of the residuals compared to the variance of the measured/observed data (Nash & Sutcliffe, 1970). Visually, the

NSE shows how well the observed versus simulated data fit on a 1:1 line.

595

$$NSE = 1 - \frac{\sum_{i=1}^{N}(P_i - O_i)^2}{\sum_{i=1}^{N}(O_i - \overline{O})^2} \qquad \text{eq. 5}$$

where $\overline{O}$ is the average value of O_i. To compute the Kling-Gupta Efficiency (KGE):

600

$$KGE = 1 - ED, \qquad \text{eq. 6}$$

$$ED = \sqrt{(r-1)^2 + \left(\frac{\sigma_P}{\sigma_O} - 1\right)^2 + \left(\frac{\mu_P}{\mu_O} - 1\right)^2}$$

where r is the linear correlation coefficient between predictions and observations. The purpose of the KGE metric is to reach

a balance between optimal conditions of modeled and observed quantities being perfectly correlated (i.e., $r = 1$), with the

605 same variance (σ_p / σ_o = 1) and minimizing model output bias (μ_p / μ_o = 1). The Kling-Gupta Efficiency (KGE) is based on

a decomposition of NSE into separate components (correlation, variability bias, and mean bias), and tries to improve on NSE

weaknesses (Knoben et al., 2019). Like NSE, KGE = 1 is a perfect fit between model simulations/predictions and

observations/measurements. However, NSE and KGE values cannot be directly compared because each metric is influenced by the coefficient of variation of the observed time series (Knoben et al., 2019).

610 The Willmott index of agreement, *d*, ranging from 0 to -1, is defined as a standardized measure of model prediction error where a value of 1 is a perfect agreement between measured and predicted values, and a value of 0 indicates no agreement.

$$d = 1 - \frac{\Sigma_{i=1}^{N}(P_i - O_i)^2}{\Sigma_{i=1}^{N}(|P_i - \overline{O}| + |O_i - \overline{O}|)^2} \qquad \text{eq.7}$$

615 The Akaike Information Criterion (AIC) is a selection method used to compare several models to find the best approximating model for the data set of interest (Akaike et al., 1973; Banks & Joyner, 2017; Portet, 2020). For details on the mathematical derivation and application of AIC, please see Banks & Joyner (2017), Portet (2020) and Piotrowski et al. (2021). The AIC equation version shown was developed for the least-squares approach (Anderson & Burnham, 2004):

620 $$AIC \; = \; N \cdot ln(MSE) + \; 2 \cdot K \qquad \text{eq.8}$$

where *N* is the number of samples, *K* is the number of model parameters + 1, and *MSE* is obtained by the model, for the respective dataset, per stream (Piotrowski et al., 2021). The Bayesian Information Criterion (BIC) was developed for studies where model errors are assumed to follow a Gaussian distribution (Faraway & Chatfield, 1998; Piotrowski et al., 2021). For 625 other versions of BIC, please see Faraway & Chatfield, 1998.

$$BIC \; = \; N \cdot ln(MSE) + \; Kln(N) \qquad \text{eq.9}$$

Unlike other performance metrics, the AIC and BIC are unique in their ability to penalize the number of parameters used by 630 a model, thus favouring more parsimonious models. For both the AIC and BIC, lower values of criterion point to a better model (Piotrowski et al., 2021).

3.4 Performance Metrics for Most-Cited ML Statistics

Reviewing ML studies focused on SWT modeling (Table S1, S2), the most-cited performance metrics were: RMSE (42 citations), *r* and R^2 (28), NSE (24), and MAE (18). As part of our efforts to propose guidelines for easier comparison of ML 635 performance across SWT studies, we identified the range in reported values for these four most cited metrics and show the spread of values in the training/calibration, testing and validation phases in box plot form.

We begin with the standard regression and dimensionless statistics, R^2 and NSE, both of which have an optimal value of 1. We note that for the 11 studies that used Pearson's *r* (see Table S1), and given that *r* and R^2 are directly related, we converted *r* to R^2 for ease of comparison on fig. 1. Figure 1 shows the median R^2 per ML model per model phase for the cited

640 publications. For example, Foreman et al. (2001) used an ANN to model SWT in the Fraser Watershed in British Columbia, Canada. Their model estimated 1995–1998 tributary and headwater temperatures and reported a median R^2 (fig. 1) of 0.93 for the training/calibration phase. Over the review period, R^2 range (2001–2024) was 0.65–1.00. We note that for process-based modeling, acceptable R^2 values start around $R^2 \sim 0.50$ (Moriasi et al., 2007). In stark contrast, ML models published between 2000–2024 exhibited significantly higher R^2 values with a median of $R^2 \sim 0.93$, across 28 studies (fig. 1).

645 Unlike the R^2 metric, NSE was not used as a metric in ML studies of SWT between 2000 and 2010 (fig. 2). The first ML study to use NSE was St. Hilaire et al., (2011) to analyse SWT in Catamaran Brook, a small catchment in New Brunswick, Canada. Figure 2 shows that the NSE range reported by studies using ML for SWT was between 0.35–1.00 over the reviewed period (2000–2024). Like R^2, NSE published values are high compared to traditional models (Moriasi et al., 2007, 2015), with a median NSE of 0.93 across 24 studies (fig. 2).
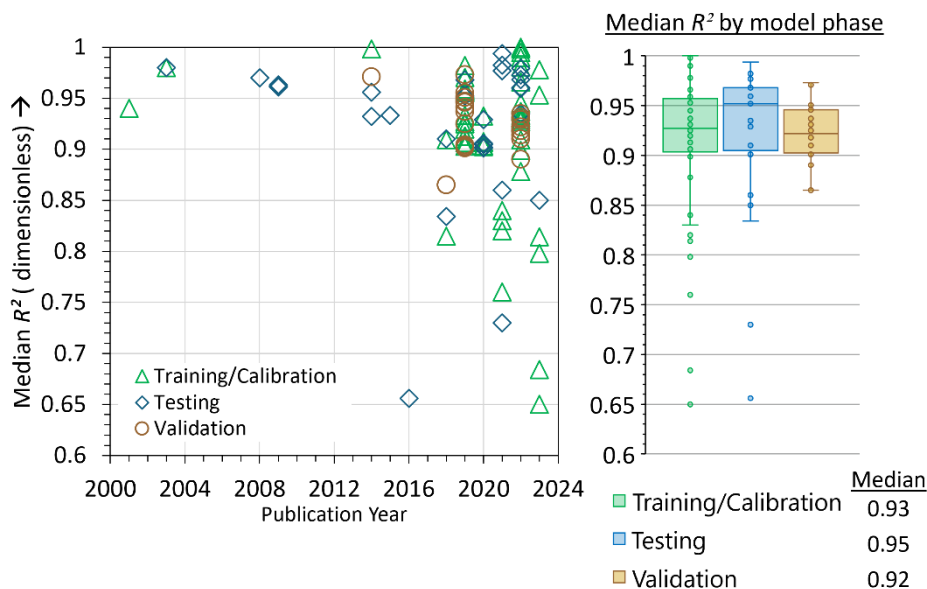
650

Figure 1. Median R^2 (dimensionless) values from published literature for training/calibration, testing, and validation phases of model evaluation.
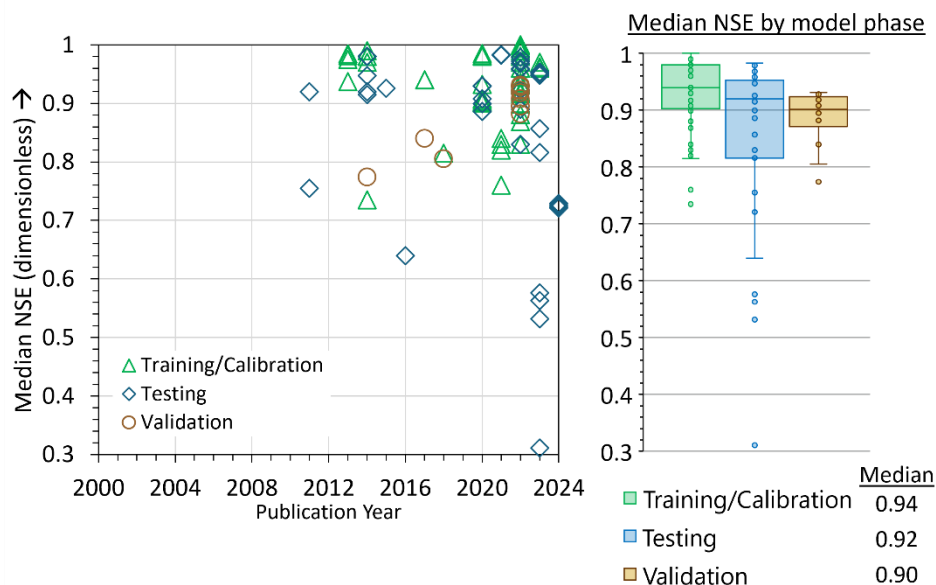
Figure 2. Median NSE (dimensionless) values from published literature for training/calibration, testing, and validation phases of model evaluation.
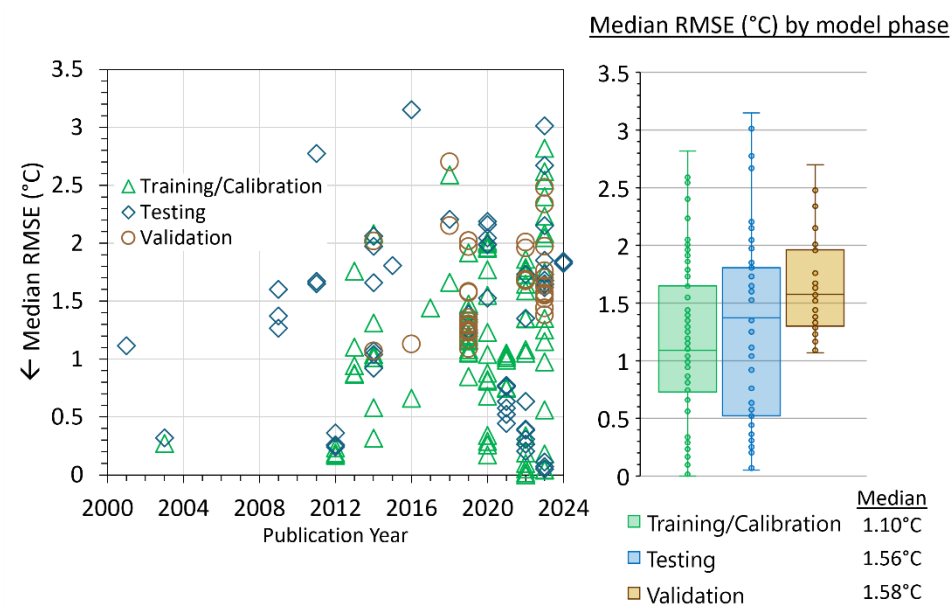
Figure 3. Median RMSE (°C) values from published literature for training/calibration, testing, and validation phases of model evaluation.

Figure 3 shows the median RMSE (°C) and fig. 4 shows the median MAE (°C) per ML model per model phase for each publication. RMSE (°C) and MAE (°C) are popular error indices used in model evaluation because the metrics show error in the units of the data of interest (i.e., °C), which helps analysis of the results. RMSE and MAE values equal to 0 are a perfect

fit. Over the review period, median RMSE (fig. 3) ranged from 0.0002–3.15 °C. The median RMSE values was 1.33 °C across 42 studies (fig. 3). Figure 4 shows that between 2000–2012, MAE was not used as a metric in ML studies of SWT. The first ML study to use MAE for SWT modeling was Grbic et al. (2013), where the Gaussian process regression (GPR)
665 ML approach was compared with field observations of SWT from the Drava River in Croatia, to assess the feasibility of model development in SWT prediction. In contrast to RMSE, the MAE range (fig. 4) was 0.14–2.19 °C. The median MAE overall was 1.09 °C respectively across 18 studies (fig. 4).
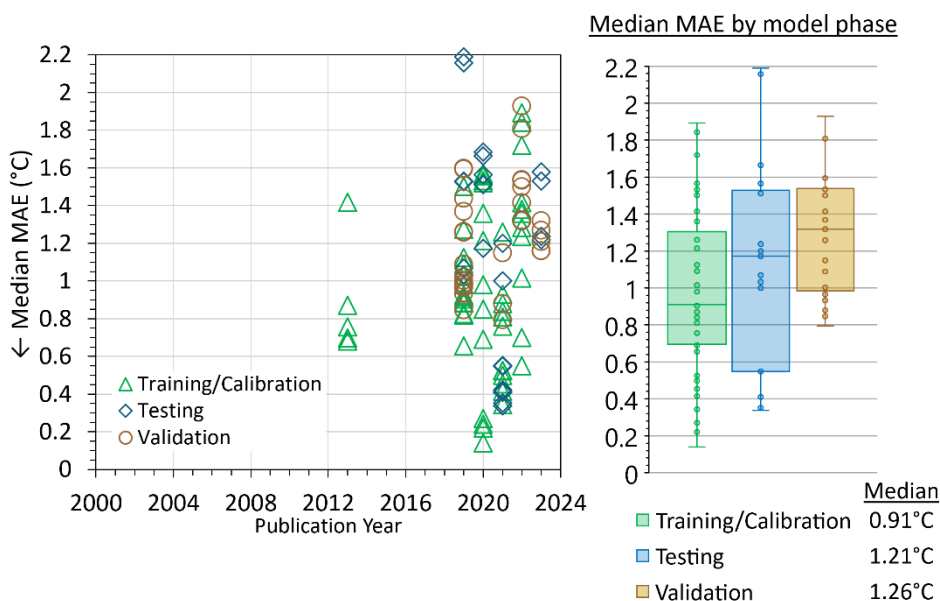
Figure 4. Median MAE (°C) values from published literature for training/calibration, testing, and validation phases of model
670 **evaluation.**

Table 1. Average, median, maximum, and minimum RMSE (°C) for studies grouped by local/watershed and regional/CONUS spatial scales.

	Local/Watershed (< 100 km² area)	Regional/CONUS (> 100 km² area)
Number of data points	899	1291
Average	1.51	1.55
Median	1.38	1.42
Maximum	5.170	4.387
Minimum	0.038	0.0002

675

3.5 Spatial Scale

We examined the data for the possible influence of spatial scale on the most-cited performance metric, RMSE, by grouping publications into two spatial categories: local, which included studies that focused on point to plot, specific sites, and small watersheds less than ~100 km^2 in area (about the size of a HUC-08), and regional, which included everything over ~100 km^2 in area. For this analysis, all RMSE values reported by publications were compiled into a table (not shown) and classified as belonging to either the local/watershed or regional/CONUS scale. A comparison of the data found that the average RMSE was similar for the local (~ 1.51 °C) and regional (~ 1.55 °C) categories. The median regional RMSE was slightly better than the local RMSE (~ 0.04 °C), but arguably within a standard of error. The local/watershed category had a higher maximum and minimum RMSE than those reported for the regional category. Overall, neither category appeared significantly better or worse than the other.

Table 2. Suggested ratings for performance metrics (median) using metrics published by ML studies examining SWT.

	R^2			NSE		
Rating	Training	Testing	Validation	Training	Testing	Validation
Very Good (>)	0.99	0.99	0.96	0.99	0.97	0.93
Good (range)	0.92 - 0.99	0.92 - 0.99	0.92 - 0.96	0.92 - 0.99	0.88 - 0.97	0.88 - 0.94
Satisfactory (range)	0.85 - 0.92	0.86 - 0.92	0.88 - 0.92	0.84 - 0.92	0.70 - 0.88	0.83 - 0.88
Unsatisfactory (<)	0.85	0.86	0.88	0.84	0.61	0.83
	RMSE (°C)			MAE (°C)		
Rating	Training	Testing	Validation	Training	Testing	Validation
Very Good (>)	0.25	0.22	1.16	0.33	0.42	0.86
Good (range)	1.34 - 0.25	1.42 - 0.22	1.81 - 1.16	1.18 - 0.33	1.12 - 0.42	1.32 - 0.86
Satisfactory (range)	2.43 - 1.34	2.70 - 1.46	2.45 - 1.81	1.70 - 1.01	1.97 - 1.19	1.79 - 1.32
Unsatisfactory (<)	2.43	2.70	2.45	1.70	1.97	1.79

3.6 Temporal Scale

Across studies, there was large variability in the focus of temporal scales and use. For example, some studies used data collected at 5–15 minute intervals to simulate SWT at daily or weekly intervals for an abbreviated period (Risley et al., 2003; Hong and Bhamidimarri, 2012). Other studies used data collected at hourly, daily, weekly, or monthly intervals (Foreman et al., 2001; Sivri et al., 2007; Temizyurek and Dadaser-Celik, 2018) for periods of record spanning weeks (Lu and Ma, 2020; Abdi et al., 2021) to several decades (Cole et al., 2014; Weierbach et al., 2022; Heddam et al., 2022; Topp et al., 2023; Rehana and Rajesh, 2023), to simulate SWT. Concurrently, output for studies was then provided at resolutions ranging from hourly to monthly periods for the past, present or future. Given the use of study-specific temporal outputs and the limited amount of reported peer-reviewed model performance data at the temporal scales used by researchers, it was difficult to conduct statistical comparisons for temporal scales, so they are not further discussed in this review. We strongly suggest to

researchers that metrics be made available at the temporal scale of interest (and not just for the overall model) in appendices or supplementary information to encourage more comparison across studies.

4 Discussion

4.1 Model Evaluation Ratings

From our review of RMSE, R^2, NSE, and MAE, we compiled ratings for ML performance metrics that should be used to cross-compare ML performance across SWT studies. From table S2, we note that there was not a consistent way of reporting training/validation/testing percentages, for example, some studies only reported performance metrics for one modeling phase (i.e., training), while others used the words "testing" and "validation" interchangeably, which could affect interpretation of model performance (Laanaya et al., 2017; Voza and Vuković, 2018; Hani et al., 2023). Additionally, others stated information not by percentages but for either entire time periods or separately, by years (i.e., training 2 years, testing 1 year, validation 1 year), which can make comparisons challenging. Despite all the different ways that researchers chose to compile performance metrics, most models had strong metrics, which can be seen from our calculated ratings for performance metrics shown on table 2. We argue that the definitions of satisfactory, good, and very good be updated to reflect the inherent capability of a ML algorithm to fit the input data more successfully than other model types, such as statistical models and process-based models. For example, R^2 values from ML-SWT studies that may appear to be very good, such as $R^2 \sim 0.91$, should be considered satisfactory given the context of the performance metrics published in ML-SWT literature. For table 2, review of the literature informed the performance ratings. The very good and unsatisfactory ranges were calculated from the box plots by identifying the two-thirds distance from the upper (or lower) quartile to the respective extreme whisker. This calculation identifies the ~8% of the data that is relatively closest to the minimum or maximum values of the box plots, indicating a very good or unsatisfactory value. For table 2, the separation between the satisfactory range and the good range was denoted as the halfway value between very good and unsatisfactory. The purpose of these guidelines is to serve as a reference for SWT studies looking to understand and consider ML performance relative to other SWT-ML studies.

4.2 ML Use for Knowledge Discovery

It has been suggested that the increasingly prominent use of ML for hydrological predictions points to a paradigm shift, one where the adoption of ML in most if not all future physical hydrologic modeling appears certain (Xu & Liang, 2021; Varadharajan et al., 2022). As physical scientists try to stay afloat in a sea of ML algorithm options and processes, there is a critical need to examine how "newer" tools such as ML are improving our understanding of the natural world. Our review finds that ML studies examining SWT have been conducted from a computational perspective, one with a focus on comparing techniques and performance as opposed to explaining the nature of SWT dynamics or influencing processes.

From a computational perspective, the use of ML in SWT modeling has led to improvements in pattern identification (i.e., release of water from reservoirs; see Jiang et al., 2022) and examination of climate events (i.e., extreme droughts; see Qiu et al., 2020), with the aid of observations and remote sensing data. The use of ML for estimating hydrologic variables (i.e., precipitation, snow water equivalent, and evapotranspiration) and approximating hydrologic processes (i.e., runoff generation) has also become increasingly common due to the ML's ability to use many inputs without the bounds of preexisting relationships (Xu & Liang, 2021). In addition, hybridizations that couple ML models (i.e., WT-LSTM, K-nn with LSTM; Rehana and Rajesh, 2023) or couple ML with process-based models (SNTEMP-LSTM, Rahmani et al., 2023) show potential for outperforming extensively calibrated hydrologic models, especially where physical constraints can be introduced (Rahmani et al., 2023).

Recent studies (Rahmani et al., 2023; Wade et al., 2023), have tried to infer drivers of SWT regimes by accounting for some level of physics. Compounding the challenge of applying physical laws without negatively affecting the performance of a ML model, is the problem that the ML model itself is not immune to the difficulties met by statistical and process-based models such as: data uncertainties, parameter uncertainties, and equifinality (Beven, 2020; Varadharajan et al., 2022). These uncertainties, coupled with the alarming trend of consistently high marks of the performance metrics discussed here, point to an imperative need to reevaluate how best to use ML in a manner that addresses knowledge gaps of physical systems instead of perfecting performance that is unlikely to be insightful for physical processes and trends. Our review of the literature and analysis of the performance data agrees with discussion by Beven (2020), who examined the future of hydrological sciences with ML, and posed several important questions regarding better use of ML models for scientific inquiry.

5 Conclusion

While initial examination of SWT began with statistical and process-based modeling many decades ago, there is now a strong interest within the hydrology community to use ML across the board to further our understanding of hydrologic causes and effects. Indeed, extensive progress has been made in using ML for SWT modeling solely in the last quarter century (2000–2024). As discussed in this review, applications of ML in SWT modeling have ranged from the local to the continental scale, as well as from the short-term period of hours to the longer-term period of decades.

In this review, we examined published literature that used ML for SWT modeling and provided a range of background information on the ML models used in these studies. Additionally, we compiled reported ML performance metrics and compare those most cited -- RMSE, R^2, NSE and MSE. We find that ML performance metrics surpass all our pre-conceived notions of what makes a very good vs. satisfactory model. We argue that as a scientific community, we need to redefine model success in the face of ML's consistently robust performance, or at the very least, hold ML to a separate, higher standard when comparing ML to physically based and statistically based models. To aid in re-defining standards, we introduce updated designations (for ML studies only) of very good, good, satisfactory, etc. performance metrics as derived from the literature. In addition to levelling the playing field when comparing ML results to process-based and statistically

765 based models, we assert that raising the performance bar could also strengthen user confidence in ML-models to the point that their consideration in decision-relevant predictions becomes more widely trusted and accepted.

Finally, our review finds that the increased accessibility to ML and its use in SWT modeling has yet to lead to better physical understanding of SWT causes and effects. Over the past 24 years, the focus on desired accuracy and performance metrics has overpowered much-needed trade-offs that earlier models of the 20th century considered, such as process complexity (scale,

770 heterogeneity, generalizability), knowledge discovery, timeliness, and basic public understanding. Given our knowledge that most ML models consistently perform at a higher level, we believe it is time to take a step back and purposefully consider more thoughtful creation and purposefulness of ML models for the goal of decision-relevant predictions that include risk-mitigation, water resource planning and process understanding of stream water temperature influencers and effects.

6 Code Availability

775 Computer code was not used to conduct this review.

7 Data Availability

All data was obtained from the cited publications. Data used for figures 1 to 4 and tables 1 and 2 are available online at CUAHSI HydroShare: https://www.hydroshare.org/resource/ad22cab56ea84b3f99a7b9557c4adfa8/

8 Supplement link

780 Copernicus will provide.

9 Author contribution

C.R. Corona contributions included: conceptualization, data curation, formal analysis, investigation, methodology, validation, visualization, writing – original draft preparation and writing – review & editing. T.S. Hogue contributions included: conceptualization, funding acquisition, methodology, project administration, resources, supervision, writing –

785 review & editing.

10 Competing interests

The authors declare that they have no conflict of interest.

11 Disclaimer

This manuscript and related items of information have not been formally disseminated by NOAA, and do not represent any
790   agency determination, view, or policy.

12 Acknowledgements

This project was supported by the NOAA Cooperative Institute for Research to Operations in Hydrology. Funding was
awarded to Cooperative Institute for Research to Operations in Hydrology (CIROH) through the NOAA Cooperative
Agreement with The University of Alabama (NA22NWS4320003).

795   ## 13 References

Abdi, R., Rust, A., & Hogue, T. S. (2021). Development of a multilayer deep neural network model for predicting hourly
river water temperature from meteorological data. Frontiers in Environmental Science, 9, 738322.
https://doi.org/10.3389/fenvs.2021.738322

Ahmadi-Nedushan, B., St-Hilaire, A., Ouarda, T. B. M. J., Bilodeau, L., Robichaud, É., Thiémonge, N., & Bobée, B. (2007).
800   Predicting river water temperatures using stochastic models: case study of the Moisie River (Québec, Canada). Hydrological
Processes, 21(1), 21–34. https://doi.org/10.1002/hyp.6353

Akaike, H., Petrov, B. N., & Csaki, F. (1973). Information theory and an extension of the maximum likelihood principle.
Second International Symposium on Information Theory, 267–281.

Anderson, D., & Burnham, K. (2004). Model selection and multi-model inference. Second. NY: Springer-Verlag, 63(2020),
805   10.

Anmala, J., & Turuganti, V. (2021). Comparison of the performance of decision tree (DT) algorithms and extreme learning
machine (ELM) model in the prediction of water quality of the Upper Green River watershed. Water Environment Research,
93(11), 2360–2373. https://doi.org/10.1002/wer.1642

Banks, H. T., & Joyner, M. L. (2017). AIC under the framework of least squares estimation. Applied Mathematics Letters,
810   74, 33–45. https://doi.org/10.1016/j.aml.2017.05.005

Barbarossa, V., Bosmans, J., Wanders, N., King, H., Bierkens, M. F. P., Huijbregts, M. A. J., & Schipper, A. M. (2021).
Threats of global warming to the world's freshwater fishes. Nature Communications, 12(1), 1701.
https://doi.org/10.1038/s41467-021-21655-w

Bartholow, J. M. (1989). Stream temperature investigations: field and analytical methods (Vol. 89). US Fish and Wildlife
815   Service. Retrieved from https://www.krisweb.com/biblio/gen_usfws_bartholow_1989_br8917.pdf

Bengio, Y., Simard, P., & Frasconi, P. (1994). Learning long-term dependencies with gradient descent is difficult. IEEE
Transactions on Neural Networks, 5(2), 157–166.

Benyahya, L., Caissie, D., St-Hilaire, A., Ouarda, T. B. M. J., & Bobée, B. (2007). A Review of Statistical Water Temperature Models. Canadian Water Resources Journal, 32(3), 179–192. https://doi.org/10.4296/cwrj3203179

820   Beven, K. (2020). Deep learning, hydrological processes and the uniqueness of place. Hydrological Processes, 34(16), 3608–3613. https://doi.org/10.1002/hyp.13805

Breiman, L. (2001). Random forests. Machine Learning, 45, 5–32.

Brown, G. W. (1969). Predicting Temperatures of Small Streams. Water Resources Research, 5(1), 68–75. https://doi.org/10.1029/WR005i001p00068

825   Cairns, J., Jr., Heath, A. G., & Parker, B. C. (1975). Temperature influence on chemical toxicity to aquatic organisms. Journal (Water Pollution Control Federation), 47(2), 267–280.

Caissie, D., El-Jabi, N., & St-Hilaire, A. (1998). Stochastic modeling of water temperatures in a small stream using air to water relations. Canadian Journal of Civil Engineering, 25.

Chang, H., & Psaris, M. (2013). Local landscape predictors of maximum stream temperature and thermal sensitivity in the

830   Columbia   River   Basin,   USA.   Science   of   The   Total   Environment,   461–462,   587–600. https://doi.org/10.1016/j.scitotenv.2013.05.033

Chen, Y. D., Carsel, R. F., McCutcheon, S. C., & Nutter, W. L. (1998). Stream temperature simulation of forested riparian areas: I. Watershed-scale model development. Journal of Environmental Engineering, 124(4), 304–315.

Chen, Y. D., McCutcheon, S. C., Norton, D. J., & Nutter, W. L. (1998). Stream temperature simulation of forested riparian

835   areas: II. Model application. Journal of Environmental Engineering, 124(4), 316–328.

Chenard, J., & Caissie, D. (2008). Stream temperature modeling using artificial neural networks: application on Catamaran Brook, New Brunswick, Canada. Hydrological Processes, 22(17), 3361–3372. https://doi.org/10.1002/hyp.6928

Cho, K., van Merrienboer, B., Gulcehre, C., Bahdanau, D., Bougares, F., Schwenk, H., & Bengio, Y. (2014, September 2). Learning Phrase Representations using RNN Encoder-Decoder for Statistical Machine Translation. arXiv. Retrieved from

840   http://arxiv.org/abs/1406.1078

Cluis, D. A. (1972). Relationship Between Stream Water Temperature and Ambient Air Temperature. Hydrology Research, 3(2), 65–71. https://doi.org/10.2166/nh.1972.0004

Cole, J. C., Maloney, K. O., Schmid, M., & McKenna, J. E. (2014). Developing and testing temperature models for regulated systems: A   case   study   on   the   Upper   Delaware   River.   Journal   of   Hydrology,   519,   588–598.

845   https://doi.org/10.1016/j.jhydrol.2014.07.058

Cortes,   C.,   &   Vapnik,   V.   (1995).   Support-vector   networks.   Machine   Learning,   20(3),   273–297. https://doi.org/10.1007/BF00994018

Cover, T., & Hart, P. (1967). Nearest neighbor pattern classification. IEEE Transactions on Information Theory, 13(1), 21–27. https://doi.org/10.1109/TIT.1967.1053964

850   Dawdy, D. R., & Thompson, T. H. (1967). Digital Computer Simulation in Hydrology. Journal AWWA, 59(6), 685–688. https://doi.org/10.1002/j.1551-8833.1967.tb03398.x

Detenbeck, N. E., Morrison, A. C., Abele, R. W., & Kopp, D. A. (2016). Spatial statistical network models for stream and river temperature in New England, USA. Water Resources Research, 52(8), 6018–6040. https://doi.org/10.1002/2015WR018349

855 DeWeber, J. T., & Wagner, T. (2014). A regional neural network ensemble for predicting mean daily river water temperature. Journal of Hydrology, 517, 187–200. https://doi.org/10.1016/j.jhydrol.2014.05.035

Drainas, K., Kaule, L., Mohr, S., Uniyal, B., Wild, R., & Geist, J. (2023). Predicting stream water temperature with artificial neural networks based on open-access data. Hydrological Processes, 37(10), e14991. https://doi.org/10.1002/hyp.14991

Dugdale, S. J., Hannah, D. M., & Malcolm, I. A. (2017). River temperature modeling: A review of process-based approaches

860 and future directions. Earth-Science Reviews, 175, 97–113. https://doi.org/10.1016/j.earscirev.2017.10.009

Edinger, J. E., Duttweiler, D. W., & Geyer, J. C. (1968). The response of water temperatures to meteorological conditions. Water Resources Research, 4(5), 1137–1143.

Elman, J. L. (1990). Finding Structure in Time. Cognitive Science, 14(2), 179–211. https://doi.org/10.1207/s15516709cog1402_1

865 Fahlman, S., & Lebiere, C. (1989). The cascade-correlation learning architecture. Advances in Neural Information Processing Systems, 2.

Faraway, J., & Chatfield, C. (1998). Time Series Forecasting with Neural Networks: A Comparative Study Using the Air Line Data. Journal of the Royal Statistical Society Series C: Applied Statistics, 47(2), 231–250. https://doi.org/10.1111/1467-9876.00109

870 Feigl, M., Lebiedzinski, K., Herrnegger, M., & Schulz, K. (2021). Machine-learning methods for stream water temperature prediction. Hydrology and Earth System Sciences, 25(5), 2951–2977. https://doi.org/10.5194/hess-25-2951-2021

Fix, E., & Hodges, J. L. (1952). Discriminatory analysis: Nonparametric discrimination: Small sample performance.

Foreman, M. G. G., Lee, D. K., Morrison, J., Macdonald, S., Barnes, D., & Williams, I. V. (2000). Simulations and retrospective analyses of fraser watershed flows and temperatures. Atmosphere-Ocean, 39(2), 89–105.

875 https://doi.org/10.1080/07055900.2001.9649668

Friedberg, R. M. (1958). A Learning Machine: Part I. IBM Journal of Research and Development, 2(1), 2–13. https://doi.org/10.1147/rd.21.0002

Fuller, M. R., Detenbeck, N. E., Leinenbach, P., Labiosa, R., & Isaak, D. (2023). Spatial and temporal variability in stream thermal regime drivers for three river networks during the summer growing season. JAWRA Journal of the American Water

880 Resources Association, 1752–1688.13158. https://doi.org/10.1111/1752-1688.13158

Gers, F. A., & Schmidhuber, J. (2000). Recurrent nets that time and count. In Proceedings of the IEEE-INNS-ENNS International Joint Conference on Neural Networks. IJCNN 2000. Neural Computing: New Challenges and Perspectives for the New Millennium (pp. 189–194 vol.3). Como, Italy: IEEE. https://doi.org/10.1109/IJCNN.2000.861302

Google LLC. (2024, February 2). Bard. Large Language Model, Alphabet, Inc. Retrieved from https://bard.google.com/

885   Graf, R., & Aghelpour, P. (2021). Daily River Water Temperature Prediction: A Comparison between Neural Network and Stochastic Techniques. Atmosphere, 12(9), 1154. https://doi.org/10.3390/atmos12091154

Graf, R., Zhu, S., & Sivakumar, B. (2019). Forecasting river water temperature time series using a wavelet–neural network hybrid modeling approach. Journal of Hydrology, 578, 124115. https://doi.org/10.1016/j.jhydrol.2019.124115

Grbić, R., Kurtagić, D., & Slišković, D. (2013). Stream water temperature prediction based on Gaussian process regression.
890   Expert Systems with Applications, 40(18), 7407–7414. https://doi.org/10.1016/j.eswa.2013.06.077

Greff, K., Srivastava, R. K., Koutník, J., Steunebrink, B. R., & Schmidhuber, J. (2016). LSTM: A search space odyssey. IEEE Transactions on Neural Networks and Learning Systems, 28(10), 2222–2232.

Gupta, H. V., Sorooshian, S., & Yapo, P. O. (1999). Status of Automatic Calibration for Hydrologic Models: Comparison with Multilevel Expert Calibration. Journal of Hydrologic Engineering, 4(2), 135–143. https://doi.org/10.1061/(ASCE)1084-
895   0699(1999)4:2(135)

Hadzima-Nyarko, M., Rabi, A., & Šperac, M. (2014). Implementation of Artificial Neural Networks in Modeling the Water-Air Temperature Relationship of the River Drava. Water Resources Management, 28(5), 1379–1394. https://doi.org/10.1007/s11269-014-0557-7

Hani, I., St-Hilaire, A., & Ouarda, T. B. M. J. (2023). Machine-learning modeling of hourly potential thermal refuge area: A
900   case study from the Sainte-Marguerite River (Quebec, Canada). River Research and Applications, rra.4191. https://doi.org/10.1002/rra.4191

Hastie, T., Friedman, J., & Tibshirani, R. (2001). The Elements of Statistical Learning. New York, NY: Springer New York. https://doi.org/10.1007/978-0-387-21606-5

He, E., Xie, Y., Sun, A., Zwart, J., Yang, J., Jin, Z., et al. (2024). Fair Graph Learning Using Constraint-Aware Priority
905   Adjustment and Graph Masking in River Networks. Proceedings of the AAAI Conference on Artificial Intelligence, 38(20), 22087–22095. https://doi.org/10.1609/aaai.v38i20.30212

Hebert, C., Caissie, D., Satish, M. G., & El-Jabi, N. (2014). Modeling of hourly river water temperatures using artificial neural networks. Water Quality Research Journal, 49(2), 144–162. https://doi.org/10.2166/wqrjc.2014.007

Heddam, S., Kim, S., Danandeh Mehr, A., Zounemat-Kermani, M., Ptak, M., Elbeltagi, A., et al. (2022). Bat algorithm
910   optimised extreme learning machine (Bat-ELM): A novel approach for daily river water temperature modeling. The Geographical Journal, 189(1), 78–89. https://doi.org/10.1111/geoj.12478

Heddam, S., Ptak, M., Sojka, M., Kim, S., Malik, A., Kisi, O., & Zounemat-Kermani, M. (2022). Least square support vector machine-based variational mode decomposition: a new hybrid model for daily river water temperature modeling. Environmental Science and Pollution Research, 29(47), 71555–71582. https://doi.org/10.1007/s11356-022-20953-0

915   Hinton, G. E. (1992). How Neural Networks Learn from Experience. Scientific American, 267(3), 144–151.

Hochreiter, S., & Schmidhuber, J. (1997). Long short-term memory. Neural Computation, 9(8), 1735–1780.

Hong, Y.-S. T., & Bhamidimarri, R. (2012). Dynamic neuro-fuzzy local modeling system with a nonlinear feature extraction for the online adaptive warning system of river temperature affected by waste cooling water discharge. Stochastic Environmental Research and Risk Assessment, 26(7), 947–960. https://doi.org/10.1007/s00477-011-0543-z

920   Hsu, K., Gupta, H. V., & Sorooshian, S. (1995). Artificial neural network modeling of the rainfall-runoff process. Water Resources Research, 31(10), 2517–2530.

Huang, G.-B., Zhu, Q.-Y., & Siew, C.-K. (2006). Extreme learning machine: Theory and applications. Neurocomputing, 70(1–3), 489–501. https://doi.org/10.1016/j.neucom.2005.12.126

Irani, J., Pise, N., & Phatak, M. (2016). Clustering Techniques and the Similarity Measures used in Clustering: A Survey. 925   International Journal of Computer Applications, 134(7), 9–14. https://doi.org/10.5120/ijca2016907841

Islam, M. N., & Sivakumar, B. (2002). Characterization and prediction of runoff dynamics: a nonlinear dynamical view. Advances in Water Resources, 25(2), 179–190. https://doi.org/10.1016/S0309-1708(01)00053-7

Ivakhnenko, A. G. (1970). Heuristic self-organization in problems of engineering cybernetics. Automatica, 6(2), 207–219.

Ivakhnenko, A. G., & Ivakhnenko, G. A. (1995). The review of problems solvable by algorithms of the group method of data 930   handling (GMDH). Pattern Recognition and Image Analysis c/c of Raspoznavaniye Obrazov i Analiz Izobrazhenii, 5, 527–535.

Jaber, F., & Shukla, S. (2012). MIKE SHE: Model use, calibration, and validation. Transactions of the ASABE, 55(4), 1479–1489.

Jang, J.-S. R. (1993). ANFIS: adaptive-network-based fuzzy inference system. IEEE Transactions on Systems, Man, and 935   Cybernetics, 23(3), 665–685. https://doi.org/10.1109/21.256541

Janson, D. J., & Frenzel, J. F. (1993). Training product unit neural networks with genetic algorithms. IEEE Expert, 8(5), 26–33.

Jeong, K., Lee, J., Lee, K. Y., & Kim, B. (2016). Artificial Neural Network-based Real Time Water Temperature Prediction in the Soyang River. The Transactions of The Korean Institute of Electrical Engineers, 65(12), 2084–2093. 940   https://doi.org/10.5370/KIEE.2016.65.12.2084

Jiang, D., Xu, Y., Lu, Y., Gao, J., & Wang, K. (2022). Forecasting Water Temperature in Cascade Reservoir Operation-Influenced River with machine learning Models. Water, 14(14), 2146. https://doi.org/10.3390/w14142146

Johnson, S. L., & Jones, J. A. (2000). Stream temperature responses to forest harvest and debris flows in western Cascades, Oregon, 57.

945   Kalogirou, S. A. (2023). Solar energy engineering: processes and systems. Elsevier.

Karunanithi, N., Grenney, W. J., Whitley, D., & Bovee, K. (1994). Neural Networks for River Flow Prediction. Journal of Computing in Civil Engineering, 8(2), 201–220. https://doi.org/10.1061/(ASCE)0887-3801(1994)8:2(201)

Khosravi, M., Duti, B. M., Yazdan, M. M. S., Ghoochani, S., Nazemi, N., & Shabanian, H. (2023). Multivariate Multi-Step Long Short-Term Memory Neural Network for Simultaneous Stream-Water Variable Prediction. Eng, 4(3), 1933–1950. 950   https://doi.org/10.3390/eng4030109

Knoben, W. J. M., Freer, J. E., & Woods, R. A. (2019). Technical note: Inherent benchmark or not? Comparing Nash–Sutcliffe and Kling–Gupta efficiency scores. Hydrology and Earth System Sciences, 23(10), 4323–4331. https://doi.org/10.5194/hess-23-4323-2019

Kratzert, F., Klotz, D., Brenner, C., Schulz, K., & Herrnegger, M. (2018). Rainfall–runoff modeling using Long Short-Term
955   Memory (LSTM) networks. Hydrology and Earth System Sciences, 22(11), 6005–6022. https://doi.org/10.5194/hess-22-6005-2018

Kratzert, F., Klotz, D., Shalev, G., Klambauer, G., Hochreiter, S., & Nearing, G. (2019). Towards learning universal, regional, and local hydrological behaviors via machine learning applied to large-sample datasets. Hydrology and Earth System Sciences, 23(12), 5089–5110. https://doi.org/10.5194/hess-23-5089-2019

960   Krishnaraj, A., & Deka, P. C. (2020). Spatial and temporal variations in river water quality of the Middle Ganga Basin using unsupervised machine learning techniques. Environmental Monitoring and Assessment, 192(12), 744. https://doi.org/10.1007/s10661-020-08624-4

Krizhevsky, A., Sutskever, I., & Hinton, G. E. (2012). Imagenet classification with deep convolutional neural networks. Advances in Neural Information Processing Systems, 25.

965   LeCun, Y., Boser, B., Denker, J., Henderson, D., Howard, R., Hubbard, W., & Jackel, L. (1989). Handwritten digit recognition with a back-propagation network. Advances in Neural Information Processing Systems, 2.

LeCun, Y., Huang, F. J., & Bottou, L. (2004). Learning methods for generic object recognition with invariance to pose and lighting. In Proceedings of the 2004 IEEE Computer Society Conference on Computer Vision and Pattern Recognition, 2004. CVPR 2004. (Vol. 2, p. II–104). IEEE.

970   Legates, D. R., & McCabe, G. J. (1999). Evaluating the use of "goodness-of-fit" Measures in hydrologic and hydroclimatic model validation. Water Resources Research, 35(1), 233–241. https://doi.org/10.1029/1998WR900018

Liu, D., Xu, Y., Guo, S., Xiong, L., Liu, P., & Zhao, Q. (2018). Stream temperature response to climate change and water diversion activities. Stochastic Environmental Research and Risk Assessment, 32(5), 1397–1413. https://doi.org/10.1007/s00477-017-1487-8

975   Loh, W.-Y. (2008). Classification and Regression Tree Methods. Encyclopedia of Statistics in Quality and Reliability, 315–323.

Loinaz, M. C., Davidsen, H. K., Butts, M., & Bauer-Gottwein, P. (2013). Integrated flow and temperature modeling at the catchment scale. Journal of Hydrology, 495, 238–251. https://doi.org/10.1016/j.jhydrol.2013.04.039

Lu, H., & Ma, X. (2020). Hybrid decision tree-based machine learning models for short-term water quality prediction.
980   Chemosphere, 249, 126169. https://doi.org/10.1016/j.chemosphere.2020.126169

Maheu, A., Poff, N. L., & St-Hilaire, A. (2016). A Classification of Stream Water Temperature Regimes in the Conterminous USA. River Research and Applications, 32(5), 896–906. https://doi.org/10.1002/rra.2906

Majerska, M., Osuch, M., & Wawrzyniak, T. (2024). Long-term patterns and changes of unglaciated High Arctic stream thermal regime. Science of The Total Environment, 923, 171298. https://doi.org/10.1016/j.scitotenv.2024.171298

985 Martínez-Estudillo, A., Martínez-Estudillo, F., Hervás-Martínez, C., & García-Pedrajas, N. (2006). Evolutionary product unit based neural networks for regression. Neural Networks, 19(4), 477–486. https://doi.org/10.1016/j.neunet.2005.11.001

McCulloch, W. S., & Pitts, W. (1943). A logical calculus of the ideas immanent in nervous activity. The Bulletin of Mathematical Biophysics, 5, 115–133.

Microsoft, Inc. (2024, February 2). Copilot. Large Language Model. Retrieved from
990 https://copilot.microsoft.com/?culture=en-us&country=us

Møller, M. F. (1993). A scaled conjugate gradient algorithm for fast supervised learning. Neural Networks, 6(4), 525–533.

Moore, A. W., Schneider, J., & Deng, K. (1997). Efficient locally weighted polynomial regression predictions. Presented at the Proceedings of the 1997 International Machine Learning Conference. Morgan Kaufmann.

Moriasi, D. N., Arnold, J. G., Liew, M. W. V., Bingner, R. L., Harmel, R. D., & Veith, T. L. (2007). Model Evaluation
995 Guidelines for Systematic Quantification of Accuracy in Watershed Simulations. Transactions of the ASABE, 50(3), 885–900. https://doi.org/10.13031/2013.23153

Moriasi, D. N., Gitau, M. W., Pai, N., & Daggupati, P. (2015). Hydrologic and water quality models: Performance measures and evaluation criteria. Transactions of the ASABE, 58(6), 1763–1785.

Morse, W. L. (1970). Stream Temperature Prediction Model. Water Resources Research, 6(1), 290–302.
1000 https://doi.org/10.1029/WR006i001p00290

Morshed, J., & Kaluarachchi, J. J. (1998). Application of artificial neural network and genetic algorithm in flow and transport simulations. Advances in Water Resources, 22(2), 145–158. https://doi.org/10.1016/S0309-1708(98)00002-5

Nash, J. E., & Sutcliffe, J. V. (1970). River flow forecasting through conceptual models part I — A discussion of principles. Journal of Hydrology, 10(3), 282–290. https://doi.org/10.1016/0022-1694(70)90255-6

1005 OpenAI, Inc. (2024, February 2). ChatGPT. Large Language Model. Retrieved from https://chat.openai.com

Ouellet, V., St-Hilaire, A., Dugdale, S. J., Hannah, D. M., Krause, S., & Proulx-Ouellet, S. (2020). River temperature research and practice: Recent challenges and emerging opportunities for managing thermal habitat conditions in stream ecosystems. Science of The Total Environment, 736, 139679. https://doi.org/10.1016/j.scitotenv.2020.139679

Patra, R. W., Chapman, J. C., Lim, R. P., Gehrke, P. C., & Sunderam, R. M. (2015). Interactions between water temperature
1010 and contaminant toxicity to freshwater fish. Environmental Toxicology and Chemistry, 34(8), 1809–1817. https://doi.org/10.1002/etc.2990

Piotrowski, A. P., Napiorkowski, M. J., Napiorkowski, J. J., & Osuch, M. (2015). Comparing various artificial neural network types for water temperature prediction in rivers. Journal of Hydrology, 529, 302–315. https://doi.org/10.1016/j.jhydrol.2015.07.044

1015 Piotrowski, A. P., Napiorkowski, J. J., & Piotrowska, A. E. (2020). Impact of deep learning-based dropout on shallow neural networks applied to stream temperature modeling. Earth-Science Reviews, 201, 103076. https://doi.org/10.1016/j.earscirev.2019.103076

Piotrowski, A. P., Marzena, O., & Napiorkowski, J. J. (2021). Influence of the choice of stream temperature model on the projections of water temperature in rivers. Journal of Hydrology, (601), 21. https://doi.org/10.1016/j.jhydrol.2021.126629

1020 Poff, N. L., Tokar, S., & Johnson, P. (1996). Stream hydrological and ecological responses to climate change assessed with an artificial neural network. Limnology and Oceanography, 41(5), 857–863. https://doi.org/10.4319/lo.1996.41.5.0857

Poole, G. C., & Berman, C. H. (2001). An Ecological Perspective on In-Stream Temperature: Natural Heat Dynamics and Mechanisms of Human-Caused Thermal Degradation. Environmental Management, 27(6), 787–802. https://doi.org/10.1007/s002670010188

1025 Portet, S. (2020). A primer on model selection using the Akaike Information Criterion. Infectious Disease Modeling, 5, 111–128. https://doi.org/10.1016/j.idm.2019.12.010

Qiu, R., Wang, Y., Wang, D., Qiu, W., Wu, J., & Tao, Y. (2020). Water temperature forecasting based on modified artificial neural network methods: Two cases of the Yangtze River. Science of The Total Environment, 737, 139729. https://doi.org/10.1016/j.scitotenv.2020.139729

1030 Rabi, A., Hadzima-Nyarko, M., & Šperac, M. (2015). Modeling river temperature from air temperature: case of the River Drava (Croatia). Hydrological Sciences Journal, 60(9), 1490–1507. https://doi.org/10.1080/02626667.2014.914215

Rahmani, F., Appling, A., Feng, D., Lawson, K., & Shen, C. (2023). Identifying Structural Priors in a Hybrid Differentiable Model for Stream Water Temperature Modeling. Water Resources Research, 59(12), e2023WR034420. https://doi.org/10.1029/2023WR034420

1035 Rehana. (2019). River Water Temperature Modeling Under Climate Change Using Support Vector Regression. In S. K. Singh & C. T. Dhanya (Eds.), Hydrology in a Changing World (pp. 171–183). Cham: Springer International Publishing. https://doi.org/10.1007/978-3-030-02197-9_8

Rehana, S., & Rajesh, M. (2023). Assessment of Impacts of Climate Change on Indian Riverine Thermal Regimes Using Hybrid Deep Learning Methods. Water Resources Research, 59(2), e2021WR031347.
1040 https://doi.org/10.1029/2021WR031347

Risley, J. C., Roehl, E. A., & Conrads, P. A. (2003). Estimating water temperatures in small streams in western Oregon using neural network models (Water-Resources Investigations Report No. 02–2418) (p. 67). U.S. Geological Survey. https://doi.org/10.3133/wri024218

Risley, J. C., Constantz, J., Essaid, H., & Rounds, S. (2010). Effects of upstream dams versus groundwater pumping on
1045 stream temperature under varying climate conditions: Upstream Dam and Groundwater Pumping Impacts. Water Resources Research, 46(6). https://doi.org/10.1029/2009WR008587

Rogers, J. B., Stein, E. D., Beck, M. W., & Ambrose, R. F. (2020). The impact of climate change induced alterations of streamflow and stream temperature on the distribution of riparian species. PLOS ONE, 15(11), e0242682. https://doi.org/10.1371/journal.pone.0242682

1050 Sadler, J. M., Appling, A. P., Read, J. S., Oliver, S. K., Jia, X., Zwart, J. A., & Kumar, V. (2022). Multi-Task Deep Learning of Daily Streamflow and Water Temperature. Water Resources Research, 58(4), e2021WR030138. https://doi.org/10.1029/2021WR030138

Sahoo, G. B., Schladow, S. G., & Reuter, J. E. (2009). Forecasting stream water temperature using regression analysis, artificial neural network, and chaotic non-linear dynamic models. Journal of Hydrology, 378(3–4), 325–342.

1055 https://doi.org/10.1016/j.jhydrol.2009.09.037

Segura, C., Caldwell, P., Sun, G., McNulty, S., & Zhang, Y. (2015). A model to predict stream water temperature across the conterminous USA. Hydrological Processes, 29(9), 2178–2195. https://doi.org/10.1002/hyp.10357

Shamseldin, A. Y. (1997). Application of a neural network technique to rainfall-runoff modeling. Journal of Hydrology, 199(3–4), 272–294. https://doi.org/10.1016/S0022-1694(96)03330-6

1060 Shen, C. (2018). A Transdisciplinary Review of Deep Learning Research and Its Relevance for Water Resources Scientists. Water Resources Research, 54(11), 8558–8593. https://doi.org/10.1029/2018WR022643

Shi, X., Chen, Z., Wang, H., Yeung, D.-Y., Wong, W.-K., & Woo, W. (2015). Convolutional LSTM network: A Machine learning approach for precipitation nowcasting. Advances in Neural Information Processing Systems, 28.

Siegel, J. E., & Volk, C. J. (2019). Accurate spatiotemporal predictions of daily stream temperature from statistical models

1065 accounting for interactions between climate and landscape. PeerJ, 7, e7892. https://doi.org/10.7717/peerj.7892

Sinokrot, B. A., & Stefan, H. G. (1993). Stream temperature dynamics: Measurements and modeling. Water Resources Research, 29(7), 2299–2312. https://doi.org/10.1029/93WR00540

Sivri, N., Kilic, N., & Ucan, O. N. (2007). Estimation of stream temperature in Firtina Creek (Rize-Turkiye) using artificial neural network model.

1070 Smith, K., & Lavis, M. E. (1975). Environmental Influences on the Temperature of a Small Upland Stream. Oikos, 26(2), 228. https://doi.org/10.2307/3543713

Solomatine, D. P., Maskey, M., & Shrestha, D. L. (2008). Instance-based learning compared to other data-driven methods in hydrological forecasting. Hydrological Processes, 22(2), 275–287. https://doi.org/10.1002/hyp.6592

Souaissi, Z., Ouarda, T. B. M. J., & St-Hilaire, A. (2023). Non-parametric, semi-parametric, and machine learning models

1075 for river temperature frequency analysis at ungauged basins. Ecological Informatics, 75, 102107. https://doi.org/10.1016/j.ecoinf.2023.102107

Specht, D. F. (1991). A general regression neural network. IEEE Transactions on Neural Networks, 2(6), 568–576.

St-Hilaire, A., Morin, G., El-Jabi, N., & Caissie, D. (2000). Water temperature modeling in a small, forested stream: implication of forest canopy and soil temperature. Canadian Journal of Civil Engineering, 27, 1095–1108.

1080 St-Hilaire, A., Ouarda, T. B. M. J., Bargaoui, Z., Daigle, A., & Bilodeau, L. (2011). Daily river water temperature forecast model with a k-nearest neighbour approach. Hydrological Processes, 26(9), 1302–1310. https://doi.org/10.1002/hyp.8216

Suykens, J. A., & Vandewalle, J. (1999). Least squares support vector machine classifiers. Neural Processing Letters, 9, 293–300.

Tao, Y., Wang, Y., Rhoads, B., Wang, D., Ni, L., & Wu, J. (2020). Quantifying the impacts of the Three Gorges Reservoir
on water temperature in the middle reach of the Yangtze River. Journal of Hydrology, 582, 124476.
https://doi.org/10.1016/j.jhydrol.2019.124476

Temizyurek, M., & Dadaser-Celik, F. (2018). Modeling the effects of meteorological parameters on water temperature using
artificial neural networks. Water Science and Technology, 77(6), 1724–1733. https://doi.org/10.2166/wst.2018.058

Theurer, F. D., Voos, K. A., & Miller, W. J. (1985). Instream water temperature model. Western Energy and Land Use
Team, Division of Biological Services, Research …. Retrieved from
https://babel.hathitrust.org/cgi/pt?id=mdp.39015086455733&seq=1

Thirumalaiah, K., & Deo, M. C. (1998). Real-Time Flood Forecasting Using Neural Networks. Computer-Aided Civil and
Infrastructure Engineering, 13(2), 101–111. https://doi.org/10.1111/0885-9507.00090

Tibshirani, R. (1996). Regression Shrinkage and Selection Via the Lasso. Journal of the Royal Statistical Society: Series B
(Methodological), 58(1), 267–288. https://doi.org/10.1111/j.2517-6161.1996.tb02080.x

Tipping, M. E. (2001). Sparse Bayesian learning and the relevance vector machine. Journal of Machine Learning Research,
1(Jun), 211–244.

Topp, S. N., Barclay, J., Diaz, J., Sun, A. Y., Jia, X., Lu, D., et al. (2023). Stream Temperature Prediction in a Shifting
Environment: Explaining the Influence of Deep Learning Architecture. Water Resources Research, 59(4), e2022WR033880.
https://doi.org/10.1029/2022WR033880

Ulaski, M. E., Warkentin, L., Naman, S. M., & Moore, J. W. (2023). Spatially variable effects of streamflow on water
temperature and thermal sensitivity within a salmon-bearing watershed in interior British Columbia, Canada. River Research
and Applications, rra.4200. https://doi.org/10.1002/rra.4200

Varadharajan, C., Appling, A. P., Arora, B., Christianson, D. S., Hendrix, V. C., Kumar, V., et al. (2022). Can machine
learning accelerate process understanding and decision-relevant predictions of river water quality? Hydrological Processes,
36(4), e14565. https://doi.org/10.1002/hyp.14565

Voza, D., & Vuković, M. (2018). The assessment and prediction of temporal variations in surface water quality—a case
study. Environmental Monitoring and Assessment, 190(7), 434. https://doi.org/10.1007/s10661-018-6814-0

Wade, J., Kelleher, C., & Hannah, D. M. (2023). Machine learning unravels controls on river water temperature regime
dynamics. Journal of Hydrology, 623, 129821. https://doi.org/10.1016/j.jhydrol.2023.129821

Walker, J., & Lawson, J. (1977). Natural stream temperature variations in a catchment. Water Research, 11(4), 373–377.
https://doi.org/10.1016/0043-1354(77)90025-2

Wallace, J. B., & Webster, J. R. (1996). The role of macroinvertebrates in stream ecosystem function. Annual Review of
Entomology, 41(1), 115–139.

Ward. (1963). Annual variation of stream water temperature. Journal of the Sanitary Engineering Division, 89(6), 1–16.

Ward, J. V. (1998). Riverine landscapes: Biodiversity patterns, disturbance regimes, and aquatic conservation. Biological
Conservation, 83(3), 269–278. https://doi.org/10.1016/S0006-3207(97)00083-9

Weierbach, H., Lima, A. R., Willard, J. D., Hendrix, V. C., Christianson, D. S., Lubich, M., & Varadharajan, C. (2022). Stream Temperature Predictions for River Basin Management in the Pacific Northwest and Mid-Atlantic Regions Using Machine Learning. Water, 14(7), 1032. https://doi.org/10.3390/w14071032

Wild, R., Nagel, C., & Geist, J. (2023). Climate change effects on hatching success and embryonic development of fish: Assessing multiple stressor responses in a large-scale mesocosm study. Science of The Total Environment, 893, 164834. https://doi.org/10.1016/j.scitotenv.2023.164834

Wu, Z., Pan, S., Long, G., Jiang, J., & Zhang, C. (2019). Graph wavenet for deep spatial-temporal graph modeling. arXiv Preprint arXiv:1906.00121.

Xu, T., & Liang, F. (2021). Machine learning for hydrologic sciences: An introductory overview. WIREs Water, 8(5), e1533. https://doi.org/10.1002/wat2.1533

Yao, K., Cohn, T., Vylomova, K., Duh, K., & Dyer, C. (2015, August 25). Depth-Gated LSTM. arXiv. Retrieved from http://arxiv.org/abs/1508.03790

Zanoni, M. G., Majone, B., & Bellin, A. (2022). A catchment-scale model of river water quality by Machine Learning. Science of The Total Environment, 838, 156377. https://doi.org/10.1016/j.scitotenv.2022.156377

Zhu, S., & Piotrowski, A. P. (2020). River/stream water temperature forecasting using artificial intelligence models: a systematic review. Acta Geophysica, 68(5), 1433–1442. https://doi.org/10.1007/s11600-020-00480-7

Zhu, S., Nyarko, E. K., Hadzima-Nyarko, M., Heddam, S., & Wu, S. (2019). Assessing the performance of a suite of machine learning models for daily river water temperature prediction. PeerJ, 7, e7065. https://doi.org/10.7717/peerj.7065

Zhu, S., Heddam, S., Wu, S., Dai, J., & Jia, B. (2019). Extreme learning machine-based prediction of daily water temperature for rivers. Environmental Earth Sciences, 78(6), 202. https://doi.org/10.1007/s12665-019-8202-7

Zhu, S., Heddam, S., Nyarko, E. K., Hadzima-Nyarko, M., Piccolroaz, S., & Wu, S. (2019). Modeling daily water temperature for rivers: comparison between adaptive neuro-fuzzy inference systems and artificial neural networks models. Environmental Science and Pollution Research, 26(1), 402–420. https://doi.org/10.1007/s11356-018-3650-2

Zhu, S., Hadzima-Nyarko, M., Gao, A., Wang, F., Wu, J., & Wu, S. (2019). Two hybrid data-driven models for modeling water-air temperature relationship in rivers. Environmental Science and Pollution Research, 26(12), 12622–12630. https://doi.org/10.1007/s11356-019-04716-y